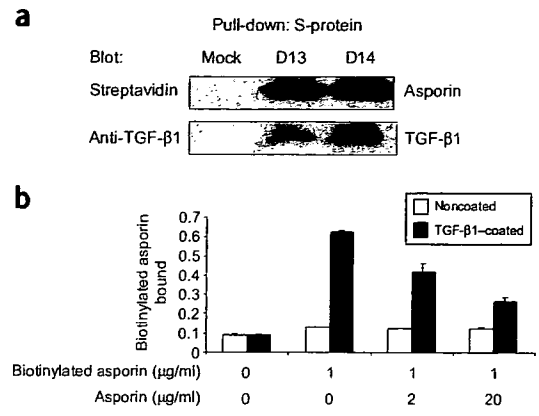

Figure 7 Asporin binds to TGF-β1 *in vitro*. (**a**) S-protein pull-down assay. *In vitro*-translated, S-tagged human asporin was incubated with recombinant human TGF-β1. Coprecipitated S-tagged biotinylated asporin was detected with streptavidin-HRP (upper panel), and TGF-β1 was detected with a biotinylated antibody to TGF-β1 (lower panel). (**b**) Solid-phase binding assay. Microplate wells coated or noncoated with recombinant human TGF-β1 were incubated with biotinylated and unlabeled recombinant mouse asporin purified from *E. coli*. Binding of biotinylated asporin to TGF-β1 was quantified by colorimetric assay at $A_{405\ nm}$ using streptavidin-HRP.

TGF-β is a multifunctional cytokine involved in numerous essential biological processes, including development, ECM synthesis, cell proliferation and differentiation, and tissue repair. Several lines of evidence suggest that TGF-β signaling is crucial for maintaining articular cartilage and preventing osteoarthritis, and that it may be a beneficial factor in cartilage repair. First, injection of TGF-β into naive murine knee joints increases the synthesis and accumulation of proteoglycan in articular cartilage[22]. Conversely, inhibition of endogenous TGF-β by treatment with recombinant soluble TGF-β type II receptor in experimental models of osteoarthritis markedly enhances proteoglycan loss in articular cartilage and reduces the thickness of articular cartilage[23]. In mouse skeletal tissue, overexpression of a dominant-negative TGF-β type II receptor promotes terminal chondrocyte differentiation and osteoarthritis[24]. Finally, targeted disruption of Smad3, the cardinal mediator of TGF-β signaling, produces degenerative joint disease mimicking human osteoarthritis, characterized by a progressive loss of articular cartilage and decreased production of proteoglycans[25]. These findings indicate that the TGF-β signal is crucial for maintaining articular cartilage and preventing osteoarthritis and that suppression of TGF-β signaling in chondrocytes probably leads to osteoarthritis.

TGF-β interacts with a number of cartilage ECM proteins, but the relationship between these proteins and TGF-β action in chondrocytes and its functional importance in chondrogenesis are unclear. But disruption of the regulatory relationship between ECM proteins and TGF-β activity contributes to several disease phenotypes. A relationship between dysregulation of TGF-β activity by fibrillin and pulmonary emphysema has been reported[26]. In addition, the SLRP family protein decorin acts as a negative regulator of TGF-β in the kidney and prevents glomerulonephritis in a rat model[27,28]. The ability of asporin to bind TGF-β directly and inhibit TGF-β–induced chondrogenesis provides another functional link between ECM proteins, TGF-β activity and disease. Our data indicate that TGF-β regulation by an ECM protein also accounts for the etiology and pathogenesis of osteoarthritis. Our data also suggest that agents controlling and modifying the TGF-β–ECM system are promising targets for treatment, offering a new therapeutic strategy for osteoarthritis.

The D-repeat polymorphic variants of asporin differ in their ability to suppress TGF-β signaling during chondrogenesis. The D repeat in asporin lies adjacent to a Zn^{2+}-binding domain that is important to conformational regulation in decorin[29]. Decorin binds fibrinogen, fibronectin and types I, IV and V collagens in a Zn^{2+}-dependent manner[30]. We therefore speculate that the D-repeat polymorphism in asporin may mediate conformational changes that consequently produce functional differences. Alternatively, the D repeat itself might affect asporin function; a D repeat contained in osteopontin functions as a Ca^{2+}-binding domain[31]. Determining structure-function relationships in asporin and assessing the contribution of the D repeat to asporin function will be the focus of future work.

The basic role of asporin in the pathogenesis of osteoarthritis remains to be examined. The reduced responsiveness to TGF-β caused by asporin may cause a mild chondrodysplasia with a consecutive osteoarthritis phenotype, with the main lesion occurring during cartilage development. Alternatively, asporin may have a major role in cartilage matrix homeostasis in the adult as a modulator of cell and ECM regeneration. There is no evidence for chondrodysplasia in our populations, and we found that asporin had a similar effect in adult articular cartilage chondrocyte as in ATDC cells. These observations support the latter hypothesis. We speculate that growth factors including TGF-β would be induced in the cellular response to tissue damage and would participate in regeneration of cartilage. In this process, asporin would act as a crucial modulator of TGF-β, fine-tuning its function. Derangement of the control mechanism (*e.g.*, too much inhibition of TGF-β activity by the disease-associated allele) would progress osteoarthritis more quickly. The allelic difference in the biological effects of asporin may result from the difference in binding intensity to TGF-β or from its effects on TGF-β receptors and not on TGF-β itself. Asporin might hinder the binding of TGF-β to its receptors or the ligand-induced dimerization of the receptors. Clarifying the mechanism would lead to the understanding of the functional link between ECM proteins, TGF-β activity and disease.

METHODS

High-density oligonucleotide microarray analysis. We carried out GeneChip analysis in accordance with a standard protocol (Affymetrix). We purchased total RNAs from osteoarthritis and normal cartilage from Direct Clinical Access and used 5–10 μg of total RNAs to prepare biotinylated cRNAs for hybridization. We hybridized biotinylated cRNAs to GeneChip Array Sets U-95 and U-133 (Affymetrix) using standard conditions. We scanned arrays with a Confocal Scanner (Molecular Dynamics) and normalized the array-hybridization signal using the median value among the signal intensities of all genes identified as 'present' by GeneChip analysis software.

Human articular cartilage samples. We obtained osteoarthritis cartilage from knee of eight individuals with osteoarthritis during surgery (total knee arthroplasty). We obtained normal cartilage from the femoral head of nine control subjects during surgery for femoral neck fractures. None of the control subjects had a clinical history of joint diseases or any radiographic sign of osteoarthritis. The samples were immediately frozen in liquid nitrogen after resection and stored at −80 °C.

Subjects. All individuals recruited for this study were Japanese and received clinical and radiographic examinations by orthopedic specialists. Osteoarthritis was diagnosed on the basis of clinical and radiographic findings. Rheumatoid arthritis and polyarthritis associated with autoimmune diseases were excluded, as were post-traumatic osteoarthritis and infection-induced osteoarthritis. Individuals who had clinical and radiographic findings suggestive of skeletal dysplasias, including overt short stature, multiple symmetric involvements of

epiphyses and a definitely positive mendelian family history, were also excluded from the study.

We recruited a population-based cohort (n = 371) from inhabitants of Miyagawa village in Mie prefecture, which is located in the middle of mainland Japan (Honshu). For each individual, we took standard three-direction (*i.e.*, antero-posterior, lateral and skyline view) knee radiographs. Using the grading system of Kellgren and Lawrence (KL grade)[2], we classified the subjects as having (2–4 KL grade; n = 137, 72% female; mean age ± s.d. = 75.3 ± 5.1 years) or not having (0–1 KL grade; n = 234, 61% female; mean age ± s.d. = 73.6 ± 5.3 years) knee osteoarthritis. We also examined clinical parameters that have been reported to confound results[3,4,32,33], including family history, body mass index and complications of clinical hand osteoarthritis (Heberden's node; **Supplementary Table 3** online).

We recruited case-control subjects from individuals who lived in or around Tokyo, also located in mainland Japan, and visited the participating clinical institutions. We studied a total of 393 individuals with knee osteoarthritis (84% female; mean age ± s.d. = 72.5 ± 7.4 years), 593 individuals with hip osteoarthritis (93% female; mean age ± s.d. = 58.3 ± 10.1 years) and 374 controls (56% female; mean age ± s.d. = 28.8 ± 11.9 years). All individuals with osteoarthritis were symptomatic and were treated in participating institutions on a regular basis. For each individual with knee osteoarthritis, we took standard three-direction knee radiographs, and for each individual with hip osteoarthritis, we took antero-posterior radiographs; we assessed JSN and osteophytes in both groups. We graded individuals with knee osteoarthritis by the JSN scale, which was described previously as a modification of KL grade[16]. We included in the case group only those individuals who had knee osteoarthritis of JSN grade three or higher. The criteria for hip osteoarthritis were described previously[34].

The study protocol was approved by the ethical committees of the participating institutions (SNP Research Center of RIKEN, Mie University, The University of Tokyo, Kyorin University, Tokyo Teishin Hospital and Tokyo Metropolitan Geriatric Hospital), and written informed consent was obtained from each participant. We obtained blood samples from the participants and prepared genomic DNA from peripheral leukocytes in accordance with standard protocols.

Genotyping of the D-repeat polymorphism and SNPs. We separated 5′-FAM–labeled PCR products containing the D-repeat polymorphisms of asporin by size on an ABI PRISM 3700 DNA Sequencer (Applied Biosystems) against the Genescan-500LIZ size standard. We collected data using GeneScan Analysis 3.5 software (Applied Biosystems), and allelic assignment was semiautomated using Genotyper 3.7 software (Applied Biosystems). We genotyped SNPs using the TaqMan assay[35].

Statistical analysis. We assessed association and Hardy-Weinberg equilibrium by the χ^2 test. We calculated odds ratios and 95% confidence intervals with respect to the minor allele compared with the major allele. We calculated LD coefficients (D′) as described previously[36]. We estimated haplotype frequencies using the expectation-maximization algorithm[37].

Cell culture and transfections. We maintained ATDC5 cells in a standard medium of Dulbecco's modified Eagle medium (DMEM)-F12 containing 5% fetal bovine serum (FBS) at 37 °C under 5% CO2. For transient transfections, we plated 5 × 10^4 cells per well in a 12-well plate and grew them continuously in standard medium containing insulin-transferrin-sodium selenite media supplement (ITS, Sigma-Aldrich). After 24 h, we transfected cells with pcDNA3.1(−)-asporin containing D13, D14, D16 or D17 using FuGENE6 (Roche) in accordance with the manufacturer's instructions. We replaced the culture medium with DMEM-F12 containing 0.2% FBS and ITS 24 h after transfection. After 12 h, we treated cells with 10 ng ml^{-1} TGF-β1 for 16 h.

For stable transfections, we plated 6 × 10^4 cells per well in a 60-mm dish and grew them continuously in standard medium. After 24 h, we transfected cells with pcDNA3.1(−)-asporin containing D13 or D14 using FuGENE6. We replaced the culture medium with DMEM-F12 containing 5% FBS and G418 (500 μg ml^{-1}) 48 h after transfection. After 7 d, we diluted cells, plated them in a 96-well plate and cloned them by limiting dilution. We evaluated *ASPN* expression using real-time PCR. We selected the three clones showing the highest levels of expression of the asporin D13 and asporin D14 mRNAs. Because these clones showed the strongest inhibition of expression of *AGC1* and *COL2A1*, we used them for all subsequent experiments.

To examine the effects of asporin on TGF-β1–induced matrix gene expression, we cultured ATDC5 cells until they reached confluence. At this point, we replaced the standard medium with DMEM-F12 containing ITS, 0.2% FBS and G418 (500 μg ml^{-1}). After 12 h, we treated cells with TGF-β1 (10 ng ml^{-1}) for 16 h. For induction of chondrogenesis, we plated 4 × 10^4 cells per well in 12-well plates and grew them continuously in DMEM-F12 containing 5% FBS, ITS and G418 (500 μg ml^{-1}) at 37 °C under 5% CO2. We replaced the growth medium every other day.

Real-time PCR. We extracted total RNAs from cartilage samples or cells using Isogen (Nippongene) and purified them using an SV-Total RNA Isolation System (Promega). We synthesized random-primed cDNA using Multiscribe reverse transcriptase (PE Applied Biosystems). We carried out real-time PCR on an ABI PRISM 7700 (Applied Biosystems) using QuantiTect SYBR Green PCR (QIAGEN) in accordance with the manufacturer's instructions.

Immunoprecipitation. We cultured ATDC5 cells stably overexpressing asporin D13 and asporin D14 in the growth medium until they were ~50% confluent. We then discarded the growth medium and cultured the cells continually for 48 h with serum-free DMEM-F12 containing ITS and G418 (500 μg ml^{-1}). We centrifuged the culture media, concentrated the supernatants (conditioned media) with Amicon Ultra-15 10,000MWCO (MILLIPORE) and incubated them (0.4 ml) with 0.5 ml of BlockAce (Dainippon Pharmaceutical), 20 μl of polyclonal rabbit antibody to mouse asporin (2229-B01; recognizes mouse and human asporin) and 50 μl of Protein A-Sepharose CL-4B (Amersham Biosciences) in a rotator at 4 °C for 18 h. We collected the immunoprecipitated complex by centrifugation and washed it five times with ice-cold Buffer SNP (1% Nonidet P-40, 150 mM NaCl and 50 mM Tris-HCl (pH 8.0)). We eluted the bound proteins with 0.1 M glycine-HCl (pH 3.0). We neutralized eluted samples with 1:10 volumes of 1 M Tris-HCl (pH 8.0), separated them by SDS-PAGE and blotted them onto PVDF membranes.

Western blotting. As a primary antibody, we used a rabbit antibody against human asporin N-terminal peptide (NSLFPTREPRSHF; 2210-B02; recognizes mouse and human asporin). The antibody was biotinylated using Biotin Labeling Kit (Roche) in accordance with the manufacturer's instructions. To visualize the immune complex we used streptavidin–horseradish peroxidase (HRP) (Roche).

Measurement of cartilage proteoglycan. After 21 d of culture, ATDC5 cells overexpressing human asporin containing D13 or D14 were fixed with methanol and stained with 0.1% alcian blue (8GX, Sigma) in 3% acetic acid for 2 d at 4 °C. After washing them three times with distilled water, we photographed cells and then extracted them with 6 M guanidine-HCl. We measured the amount of dye associated with cartilage matrix at 630 nm using Ultramark Microplate Imaging System (Bio-Rad).

Expression and purification of recombinant mouse asporin. We cloned a cDNA encoding mature (lacking pre- and propeptide) mouse asporin into a pET29b expression vector and expressed it in the *Escherichia coli* Rosetta (DE3) pLys strain. We solubilized recombinant protein from inclusion bodies, renatured it using the Protein Refolding Kit (Novagen) and purified it by gel filtration using a Superose 12 column (Amersham Pharmacia).

***In vitro* translation and S-protein pull-down assay.** S-tagged human cDNAs encoding asporin D13 or asporin D14 were transcribed and translated *in vitro* by the TNT system (Promega) in the presence of Transcend Biotin-Lysyl-tRNA in accordance with the manufacturer's instructions. For each experiment, we incubated *in vitro*–translated, S-tagged asporin (10 μl) with 0.1 μg of recombinant human TGF-β1 (Genzyme) for 1 h at 4 °C in 0.3 ml of binding buffer (50 mM Tris-HCl (pH 7.5), 150 mM NaCl, 1% Triton X-100 and Complete protease inhibitor cocktail (Roche)). We added 12.5 μl of S-protein–agarose (Novagen) to the reaction and incubated it for 30 min at room temperature. We washed precipitates three times with binding buffer and subjected them to

12.5% SDS-PAGE. We detected coprecipitated proteins by western blotting using biotinylated antibody to TGF-β1 (Genzyme) and streptavidin-HRP (R&D Systems).

Solid-phase binding assay. We coated Maxisorp ELISA plate (Nunc) wells with 100 μl of 1 μg ml^{-1} recombinant human TGF-β1 in 50 mM $NaHCO_3$ buffer (pH 9.6) at 4 °C overnight. We then blocked the wells with 200 μl of Blockace (Dainippon Pharm.) at 4 °C overnight, added unlabeled and biotinylated mouse asporin to the wells in a total volume of 100 μl of Blockace and incubated them at 4 °C overnight. We washed the wells twice with 20 mM Tris-HCl (pH 7.5), 150 mM NaCl and 0.05% Tween 20 and incubated them with streptavidin–alkaline phosphatase. After washing five times with 20 mM Tris-HCl (pH 7.5), 150 mM NaCl and 0.05% Tween 20, we assayed the bound phosphatase using Alkaline phosphatase Substrate Kit (Bio-Rad).

Accession numbers. Human asporin mRNA, NM_017680; mouse asporin mRNA, NM_025711.

Note: Supplementary information is available on the Nature Genetics website.

ACKNOWLEDGMENTS

We thank the affected individuals for participating in the study; Y. Ishii, K. Tamai, H. Ishibashi, S. Okinaga, H. Hiraoka, H. Kawaguchi, S. Saitoh, T. Kubo, Y. Takatori, H. Mototani, M. Mori, K. Yoshimura, M. Oka, M. Nakajima and K. Toyoshima for help; and A. Narita for technical assistance. This work was supported by the Japanese Millennium Project.

COMPETING INTERESTS STATEMENT

The authors declare that they have no competing financial interests.

Received 3 August; accepted 29 November 2004
Published online at http://www.nature.com/naturegenetics/

1. Felson, D.T. *et al.* The prevalence of knee osteoarthritis in the elderly: the Framingham Osteoarthritis Study. *Arthritis Rheum.* **30**, 914–918 (1987).
2. Kellgren, J.H. & Lawrence, J.S. Radiological assessment of osteoarthrosis. *Ann. Rheum. Dis.* **16**, 494–502 (1957).
3. Kellgren, J.H., Lawrence, J.S. & Bier, F. Genetic factors in generalized osteoarthrosis. *Ann. Rheum. Dis.* **22**, 237–255 (1963).
4. Spector, T.D., Cicuttini, F., Baker, J., Loughlin, J. & Hart, D. Genetic influences on osteoarthritis in women: A twin study. *BMJ* **312**, 940–943 (1996).
5. Spector, T.D. & MacGregor, A.J. Risk factors for osteoarthritis: genetics. *Osteoarthritis Cartilage* **12**, S39–S44 (2004).
6. Loughlin, J. Genetic epidemiology of primary osteoarthritis. *Curr. Opin. Rheumatol.* **13**, 111–116 (2001).
7. Loughlin, J., Dowling, B., Mustafa, Z. & Chapman, K. Association of the interleukin-1 gene cluster on chromosome 2q13 with knee osteoarthritis. *Arthritis Rheum.* **46**, 1519–1527 (2002).
8. Smith, A.J.P. *et al.* Extended haplotypes and linkage disequilibrium in the IL1R1-IL1A-IL1B-IL1RN gene cluster: association with knee osteoarthritis. *Genes Immun.* **5**, 451–460 (2004).
9. Grimaud, E., Heymann, D. & Redini, F. Recent advances in TGF-β effects on chondrocyte metabolism Potential therapeutic roles of TGF-β in cartilage disorders. *Cytokine Growth Factor Rev.* **13**, 241–257 (2002).
10. Lorenzo, P. *et al.* Identification and characterization of asporin. a novel member of the leucine-rich repeat protein family closely related to decorin and biglycan. *J. Biol. Chem.* **276**, 12201–12211 (2001).
11. Henry, S.P. *et al.* Expression pattern and gene characterization of asporin. a newly discovered member of the leucine-rich repeat protein family. *J. Biol. Chem.* **276**, 12212–12221 (2001).
12. Ameye, L. & Young, M.F. Mice deficient in small leucine-rich proteoglycans: novel *in vivo* models for osteoporosis, osteoarthritis, Ehlers-Danlos syndrome, muscular dystrophy, and corneal diseases. *Glycobiology* **12**, 107R–116R (2002).
13. Gill, M.R., Oldberg, A. & Reinholt, F.P. Fibromodulin-null murine knee joints display increased incidences of osteoarthritis and alterations in tissue biochemistry. *Osteoarthritis Cartilage* **10**, 751–757 (2002).
14. Ameye, L. *et al.* Abnormal collagen fibrils in tendons of biglycan/fibromodulin-deficient mice lead to gait impairment, ectopic ossification, and osteoarthritis. *FASEB J.* **16**, 673–680 (2002).
15. Haga, H., Yamada, R., Ohnishi, Y., Nakamura, Y. & Tanaka, T. Gene-based SNP discovery as part of the Japanese Millennium Genome Project: identification of 190,562 genetic variations in the human genome. *J. Hum. Genet.* **47**, 605–610 (2002).
16. Ikeda, T. *et al.* Identification of sequence polymorphisms in two sulfation-related genes, *PAPSS2* and *SLC26A2*, and an association analysis with knee osteoarthritis. *J. Hum. Genet.* **46**, 538–543 (2001).
17. Shukunami, C. *et al.* Chondrogenic differentiation of clonal mouse embryonic cell line ATDC5 *in vitro*:differentiation-dependent gene expression of parathyroid hormone (PTH)/PTH-related peptide receptor. *J. Cell Biol.* **133**, 457–468 (1996).
18. Shukunami, C. *et al.* Cellular hypertrophy and calcification of embryonal carcinoma-derived chondrogenic cell line ATDC5 *in vitro*. *J. Bone Miner. Res.* **12**, 1174–1188 (1997).
19. Watanabe, H., de Caestecker, M.P. & Yamada, Y. Transcriptional cross-talk between Smad, ERK1/2, and p38 mitogen-activated protein kinase pathways regulates transforming growth factor-β-induced aggrecan gene expression in chondrogenic ATDC5 cells. *J. Biol. Chem.* **276**, 14466–14473 (2001).
20. Shukunami, C., Ohta, Y., Sakuda, M. & Hiraki, Y. Sequential progression of the differentiation program by bone morphogenetic protein-2 in chondrogenic cell line ATDC5. *Exp. Cell Res.* **241**, 1–11 (1998).
21. Hildebrand, A. *et al.* Interaction of the small interstitial proteoglycans biglycan, decorin, and fibromodulin with transforming growth factor β. *Biochem. J.* **302**, 527–534 (1994).
22. van Beuningen, H.M., van der Kraan, P.M., Aruntz, O.J. & van den Berg, W.B. Transforming growth factor-β1 stimulates articular chondrocyte proteoglycan synthesis and induces osteophyte formation in the murine knee joint. *Lab. Invest.* **71**, 279–290 (1994).
23. Scharstuhl, A. *et al.* Inhibition of endogenous TGF-β during experimental osteoarthritis prevents osteophyte formation and impairs cartilage repair. *J. Immunol.* **169**, 507–514 (2002).
24. Serra, R. *et al.* Expression of a truncated, kinase-defective TGF-β type II receptor in mouse skeletal tissue promotes terminal chondrocyte differentiation and osteoarthritis. *J. Cell Biol.* **139**, 541–552 (1997).
25. Yang, X. *et al.* TGF-β/Smad3 signals repress chondrocyte hypertrophic differentiation and are required for maintaining articular cartilage. *J. Cell Biol.* **153**, 35–46 (2001).
26. Neptune, E.R. *et al.* Dysregulation of TGF-β activation contributes to pathogenesis in Marfan syndrome. *Nat. Genet.* **33**, 407–411 (2003).
27. Border, W.A. *et al.* Natural inhibitor of transforming growth factor-β protects against scarring in experimental kidney disease. *Nature* **360**, 361–364 (1992).
28. Isaka, Y. *et al.* Gene therapy by skeletal muscle expression of decorin prevents fibrotic disease in rat kidney. *Nat. Med.* **2**, 418–423 (1996).
29. Yang, V.W., LaBrenz, S.R., Rosenberg, L.C., McQuillan, D.J. & Hook, M. Decorin is a Zn^{2+} metalloprotein. *J. Biol. Chem.* **274**, 12454–12460 (1999).
30. Dugan, T.A., Yang, V.W., McQuillan, D.J. & Hook, M. Decorin binds fibrinogen in a Zn^{2+}-dependent interaction. *J. Biol. Chem.* **278**, 13655–13662 (2003).
31. Singh, K. *et al.* Calcium-binding properties of osteopontin derived from non-osteogenic sources. *J. Biochem. (Tokyo)* **114**, 702–707 (1993).
32. Meulenbelt, I. *et al.* Investigation of the association of the CRTM and CRTL1 genes with radiographically evident osteoarthritis in subjects from the Rotterdam study. *Arthritis Rheum.* **40**, 1760–1765 (1997).
33. Uitterlinden, A.G. *et al.* Adjacent genes, for COL2A1 and the vitamin D receptor, are associated with separate features of radiographic osteoarthritis of the knee. *Arthritis Rheum.* **43**, 1456–1464 (2000).
34. Mabuchi, A. *et al.* Identification of sequence polymorphisms of the *COMP* (cartilage oligomeric matrix protein) gene and association study in osteoarthrosis of the knee and hip joints. *J. Hum. Genet.* **46**, 456–462 (2001).
35. Suzuki, A. *et al.* Functional haplotypes of *PADI4*, encoding citrullinating enzyme peptidylarginine deaminase 4, are associated with rheumatoid arthritis. *Nat. Genet.* **34**, 395–402 (2003).
36. Yamada, R. *et al.* Association between a single-nucleotide polymorphism in the promoter of the human interleukin-3 gene and rheumatoid arthritis in Japanese patients, and maximum-likelihood estimation of combinatorial effect that two genetic loci have on susceptibility to the disease. *Am. J. Hum. Genet.* **68**, 674–685 (2001).
37. Excoffier, L. & Slatkin, M. Maximum-likelihood estimation of molecular haplotype frequencies in a diploid population. *Mol. Biol. Evol.* **12**, 921–927 (1995).

0013-7227/05/$15.00/0
Printed in U.S.A.

Endocrinology 146(6):2620–2628

doi: 10.1210/en.2004-1511

Insulin Receptor Substrate-1 Is Required for Bone Anabolic Function of Parathyroid Hormone in Mice

Masayuki Yamaguchi,* Naoshi Ogata, Yusuke Shinoda, Toru Akune, Satoru Kamekura, Yasuo Terauchi, Takashi Kadowaki, Kazuto Hoshi, Ung-Il Chung, Kozo Nakamura, and Hiroshi Kawaguchi

Departments of Sensory and Motor System Medicine (M.Y., N.O., Y.S., T.A., S.K., K.H., U.-I.C., K.N., H.K.) and Metabolic Diseases (Y.T., T.K.), Faculty of Medicine, University of Tokyo, Tokyo 113-8655, Japan

Bone anabolic action of PTH has been suggested to be mediated by induction of IGF-I in osteoblasts; however, little is known about the molecular mechanism by which IGF-I leads to bone formation under the PTH stimulation. This study initially confirmed in mouse osteoblast cultures that PTH treatment increased IGF-I mRNA and protein levels and alkaline phosphatase activity, which were accompanied by phosphorylations of IGF-I receptor, insulin receptor substrate (IRS)-1 and IRS-2, essential adaptor molecules for the IGF-I signaling. To learn the involvement of IRS-1 and IRS-2 in the bone anabolic action of PTH *in vivo*, *IRS-1−/−* and *IRS-2−/−* mice and their respective wild-type littermates were given daily injections of PTH (80 μg/kg) or vehicle for 4 wk. In the wild-type mice, the PTH injection increased bone mineral densities of the femur, tibia, and vertebrae by 10–20% without altering the serum IGF-I level. These stimulations were similarly seen in *IRS-2−/−* mice; however, they were markedly suppressed in *IRS-1−/−* mice. Although the PTH anabolic effects were stronger on trabecular bones than on cortical bones, the stimulations on both bones were blocked in *IRS-1−/−* mice but not in *IRS-2−/−* mice. Histomorphometric and biochemical analyses showed an increased bone turnover by PTH, which was also blunted by the IRS-1 deficiency, though not by the IRS-2 deficiency. These results indicate that the PTH bone anabolic action is mediated by the activation of IRS-1, but not IRS-2, as a downstream signaling of IGF-I that acts locally as an autocrine/paracrine factor. (*Endocrinology* 146: 2620–2628, 2005)

ANABOLIC EFFECTS of PTH on bone have attracted considerable clinical attention and led to the approval of PTH for osteoporosis treatment (1–3). Although it has been well established that intermittent administration of PTH exerts potent anabolic effects on bone in animals and humans (4), the underlying mechanism is still controversial and unclear. PTH is reported to increase production of osteoprogenitors and differentiation of osteoblasts from an existing pool of osteoprogenitors and to decrease apoptosis of preexisting osteoblasts (5–7). Accumulated evidence has shown that IGF-I is an attractive candidate as a mediator for some or all of the anabolic actions of PTH on bone, in that PTH stimulates IGF-I production by osteoblastic cells (8, 9) and IGF-1 can reproduce the effects of PTH on osteoblast proliferation, differentiation, and survival (10). From *in vitro* studies, IGF-I-blocking antibodies inhibited collagen synthesis and alkaline phosphatase (ALP) activity, as well as the expression of osteocalcin mRNA induced by PTH stimulation on osteoblasts (11, 12). Furthermore, PTH anabolic actions were suppressed when administered to IGF-I-deficient mice (13, 14), suggesting the importance of the IGF-I signaling *in vivo*.

IGF-I initiates cellular responses by binding to its cell-surface receptor tyrosine kinase IGF-I receptor, which then activates essential adaptor molecule insulin receptor substrates (IRS's) followed by downstream signaling pathways like phosphatidylinositol-3 kinase (PI3K)/Akt and MAPKs (15). The mammalian IRS family contains at least four members: ubiquitous IRS-1 and IRS-2, adipose tissue-predominant IRS-3, and IRS-4 which is expressed in the thymus, brain, and kidney. We previously reported that IRS-1 and IRS-2 are expressed in bone (16, 17). Our further studies on mice lacking the IRS-1 gene (*IRS-1−/−* mice) or the IRS-2 gene (*IRS-2−/−* mice) revealed that these knockout mice exhibited severe osteopenia with distinct mechanisms: *IRS-1−/−* mice showed a low bone turnover in which both bone formation and resorption were decreased (16), whereas *IRS-2−/−* mice showed an uncoupling status with decreased bone formation and increased bone resorption (17). It therefore seems that under physiological conditions, IRS-1 is important for maintaining bone turnover, whereas IRS-2 is important for retaining the predominance of anabolic function over catabolic function of osteoblasts.

To learn the molecular mechanism by which IGF-I leads to bone formation under the PTH stimulation, the present study investigated the role of IRS-1 and IRS-2 in mediating the anabolic effects of recombinant human PTH(1–34) on bone. We first studied the effects of PTH on the IGF-I related molecules in cultured mouse osteoblasts and examined skeletal responses to PTH in *IRS-1−/−* and *IRS-2−/−* mice.

First Published Online February 17, 2005

* Dr. Yamaguchi is deceased. Regrettably, Masayuki Yamaguchi died at much too young an age and before the publication of this paper. We dedicate this paper to him and to his family.

Abbreviations: ALP, Alkaline phosphatase; BMD, bone mineral density; GAPDH, glyceraldehyde-3-phosphate dehydrogenase; GMA, glycolmethacrylate; IRS, insulin receptor substrate; PI3K, phosphatidylinositol-3 kinase; PKA, protein kinase A; pQCT, peripheral quantitative computerized tomography; WT, wild type.

Endocrinology **is published monthly by The Endocrine Society (http://www.endo-society.org), the foremost professional society serving the endocrine community.**

Materials and Methods

Animals

Mice with the original C57BL6/CBA hybrid background were generated and maintained as reported previously (16, 17). In each experiment, homozygous wild-type (WT) and *IRS-1*−/− male mice, as well as homozygous WT and *IRS-2*−/− male mice, that were littermates generated from the intercross between heterozygous mice were compared. All mice were kept in plastic cages under standard laboratory conditions with a 12-h dark, 12-h light cycle, a constant temperature of 23 C, and humidity of 48%. The mice were fed a standard rodent diet (CE-2; CLEA Japan, Inc., Tokyo, Japan) containing 25.2% protein, 4.6% fat, 4.4% fiber, 6.5% ash, 3.44 kcal/g, 2.5 IU vitamin D_3/g, 1.09% calcium, and 0.93% phosphorus with water *ad libitum*. All animal experiments were reviewed and approved by the University of Tokyo, Faculty of Medical Animal Care and Use Committee, before the study.

Osteoblast cultures

Osteoblasts were isolated from calvariae of neonatal WT, *IRS-1*−/−, and *IRS-2*−/− littermates. Calvariae were digested for 10 min, 5 times, at 37 C in an enzyme solution containing 0.1% collagenase and 0.2% dispase. Cells isolated by the last four digestions were combined as an osteoblast population and cultured in αMEM (Invitrogen, Carlsbad, CA) containing 10% FBS (HyClone Laboratories, Inc., Logan, UT) and 50 μg/ml ascorbic acid (Sigma-Aldrich Corp., St. Louis, MO).

For real-time quantitative RT-PCR analysis, primary osteoblasts were inoculated at a density of 1×10^4 cells/well in a 24-multiwell plate, and cultured in the medium above, with or without 100 nM recombinant human PTH(1–34) (Sigma-Aldrich Corp.) for 14 d. Total RNA was extracted with an ISOGEN kit (Wako Pure Chemical Industries Ltd., Osaka, Japan), according to the manufacturer's instructions. One microgram of RNA was reverse-transcribed using a Takara RNA PCR Kit, version 2.1 (Takara Shuzo Co., Shiga, Japan), to make single-stranded cDNA. The ABI Prism Sequence Detection System 7000 and Primer Express Software (Applied Biosystems, Foster City, CA) were used for PCR amplification and quantitative analysis, respectively. For the IGF-I gene, a set of primers was designed using sequences obtained from the GenBank as follows: 5′GACAGATACARRCTGTGCTCA-3′ and 5′-CTGAAGCTTGCTAACATCGC-3′. The PCR consisted of QuantiTect SYBR Green Master Mix (QIAGEN, Tokyo, Japan), 0.3 μM specific primers, and 20 ng cDNA.

For the IGF-I protein level measurement, primary osteoblasts were cultured, as described above, for 14 d, and the free IGF-I concentration in the culture media was measured with a Non-Extraction IGF-I ELISA kit (Diagnostic Systems Laboratories, Inc., Sparks, MD).

For ALP activity measurement, primary osteoblasts were cultured in the medium above with or without 10 ng/ml recombinant mouse IGF-I (Sigma-Aldrich Corp.) and 5 nM antimouse IGF-I antibody (Sigma-Aldrich Corp.). At 14 d of culture, cells were sonicated in 10 mM Tris-HCl buffer (pH 8.0) containing 1 mM $MgCl_2$ and 0.5% Triton X-100, and ALP activity in the lysate was measured using an ALP assay kit (Wako Pure Chemical Industries Ltd.). The protein content was determined using BCA protein assay reagent (Pierce Chemical Co., Rockford, IL).

Immunoprecipitation and immunoblotting

After stimulation by 100 nM PTH for the indicated time, cultured osteoblasts were lysed with TNE buffer (10 mM Tris-HCl, 150 mM NaCl, 1% NP-40, 1 mM EDTA, 10 mM NaF, 2 mM Na_3VO_4, 1 mM aminoethylbenzenesulfonyl fluoride, and 10 μg/ml aprotinin). A part of the cell lysates (100 μg) was immunoprecipitated with an antiphosphotyrosine antibody, an antimouse IGF-I receptor antibody, an antimouse insulin receptor antibody, an antimouse IRS-1 antibody, or an antimouse IRS-2 antibody (all from Upstate Biotechnology, Inc., Waltham, MA) conjugated to protein G-Sepharose (Invitrogen) for 4 h at 4 C. The cell lysates with or without the immunoprecipitation that contained an equivalent amount of protein (20 μg) were electrophoresed by 8% SDS-PAGE and transferred to nitrocellulose membrane. After blocking with 5% BSA solution, they were incubated with the antibodies above, and the immunoreactive bands were stained using the ECL chemiluminescence reaction (Amersham, Arlington Heights, IL). The intensity of each band was measured by densitometry (Bio-Rad Laboratories, Inc., Richmond, CA) and was expressed as the mean value of five independent experiments.

PTH treatment on mice

IRS-1−/− mice and their littermates and *IRS-2*−/− mice and their littermates (males, all n = 10) received either PTH (80 μg/kg body weight) or vehicle (PBS) by sc injection every day for 4 wk beginning at 10 wk of age. Blood samples were collected by heart puncture under nembutal (Dainippon Pharmaceutical Co., Ltd., Osaka, Japan) anesthesia before being killed. For radiological and histological analyses, animals were killed after 4 wk of PTH treatment by diethylether. The right femurs and tibiae were obtained for bone densitometry, and the left femurs and tibiae for peripheral quantitative computerized tomography (pQCT) and histological analyses, respectively. Lumbar vertebral bodies from L2–L5 were also obtained for bone densitometry.

Bone densitometry and pQCT

Bone mineral density (BMD; milligrams per square centimeter) of the right femur, tibiae, and L2–L5 vertebral bodies was determined using dual-energy x-ray absorptiometry (PIXImus Mouse Densitometer; Lunar Corp., Madison, WI) according to the manufacturer's instructions. Computerized tomography was performed with a pQCT analyzer (XCT Research SA+; Stratec Medizintechnik GmbH, Pforzheim, Germany) operating at a resolution of 80 μm. Metaphyseal pQCT scans of the left femurs were performed to measure the trabecular volumetric BMD. The scan was positioned in the metaphysis at 1.2 mm proximal from the distal growth plate. Because this area contains trabecular and cortical bones, the trabecular bone region was defined by setting the threshold to 395 mg/cm^3. Middiaphyseal pQCT scans of the left femurs were performed to determine the cortical thickness. The middiaphyseal region of femurs in mice contains mostly cortical bone. The cortical bone region was defined by setting the threshold to 690 mg/cm^3. The interassay coefficients of variation for the pQCT measurements were less than 2%.

Histological analyses

For the assessment of dynamic histomorphometric indices, mice were injected with calcein (16 mg/kg body weight) sc at 10 d and 3 d before being killed, after which the left tibiae were excised and fixed with ethanol, and the undecalcified bones were embedded in glycolmethacrylate. Three-micrometer sagittal sections from the proximal parts of tibiae were stained with toluidine blue and were visualized under fluorescent light microscopy for calcein labeling. The specimens were subjected to histomorphometric analyses using a semiautomated system (Osteoplan II; Carl Zeiss, Oberkochen, Germany), and measurements were made at ×400 magnification. Parameters for the trabecular bone were measured in an area 1.2 mm in length, from 250 μm below the growth plate at the proximal metaphysis of the tibiae. Nomenclature, symbols, and units are those recommended by the Nomenclature Committee of the American Society for Bone and Mineral Research (18).

Serum biochemical assays

For serum IGF-I levels, acid ethanol extraction was used to remove the IGF-binding proteins, and the extracted samples were assayed for IGF-I with a RIA kit from Nichols Institute Diagnostics (San Juan Capistrano, CA). Serum osteocalcin levels were determined by using the competitive RIA kit (Biomedical Technologies, Stoughton, MA). The sensitivity of the assay was 19 ng/ml, and the interassay and intraassay coefficients of variation were less than 10%. Serum ALP activity was determined by liquitech ALP kit (Roche Diagnostics, Basel, Switzerland) with an autoanalyzer (type 7170; Hitachi High-Technologies Corporation, Tokyo, Japan). ALP activity of the blood samples was expressed as nanomoles per minute and per milligram of protein.

Statistical analysis

Means of groups were compared by ANOVA, and significance of differences was determined by *post hoc* testing using Bonferroni's method.

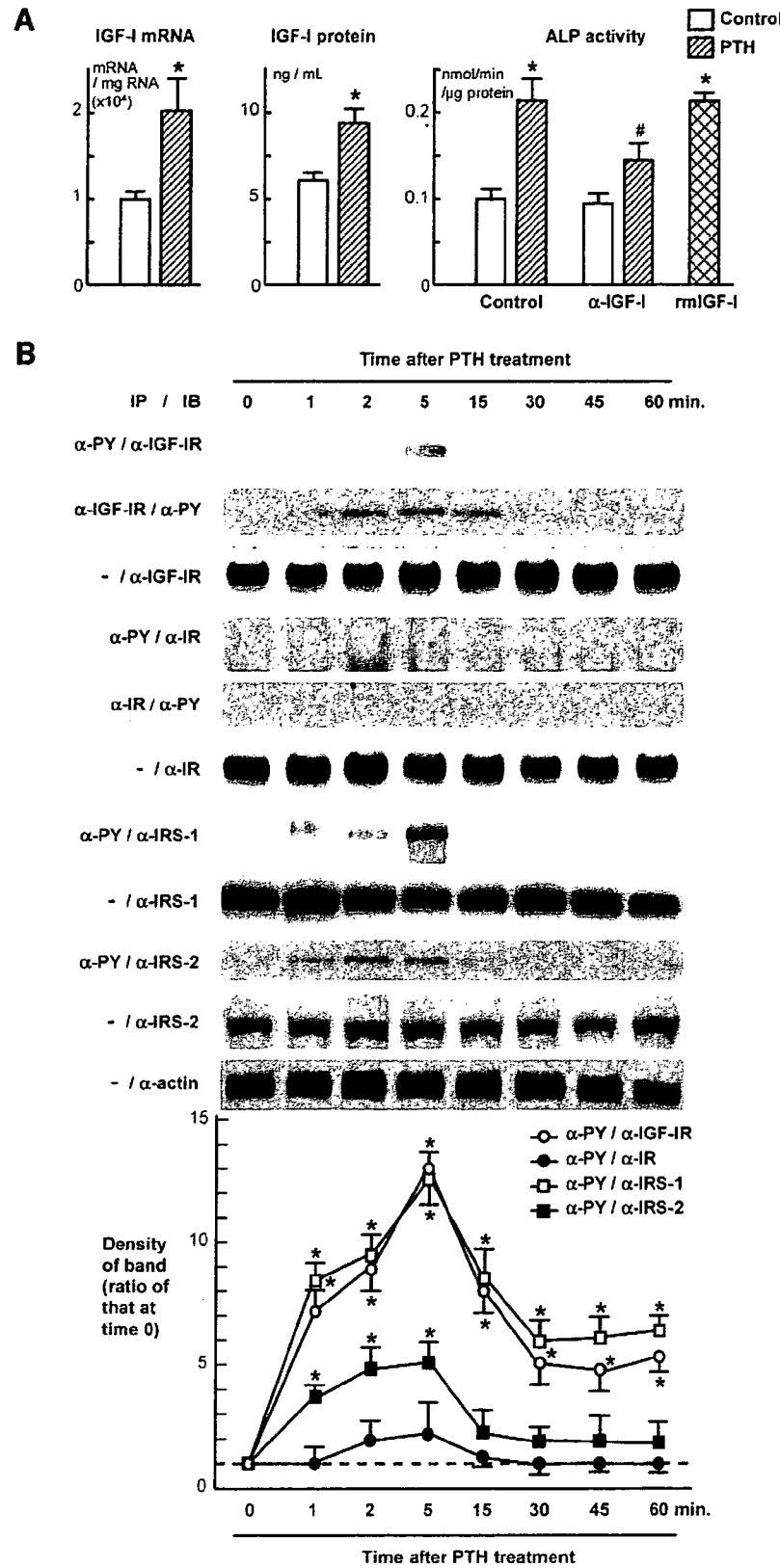

FIG. 1. Effects of PTH on cultured osteoblasts isolated from neonatal mouse calvariae. A, IGF-I mRNA level determined by real-time quantitative RT-PCR (*left*), IGF-I protein level in the culture medium (*middle*), and ALP activity in the cell lysate (*right*) in the primary calvarial osteoblast culture in the presence and absence of PTH (100 nM), an antibody against IGF-I (α-IGF-I, 5 nM), and recombinant mouse IGF-I (rmIGF-I, 10 ng/ml) for 2 wk. Data are expressed as means (*bars*) ± SEM (*error bars*) for eight wells per group. *, Significant increase compared with the control culture, $P < 0.01$; #, significant inhibition by α-IGF-I, $P < 0.05$. B, Protein levels by immunoprecipitation (IP) and immunoblotting (IB) of IGF-I receptor, insulin receptor, IRS-1, and IRS-2 with or without phosphorylation in osteoblasts cultured with PTH (100 nM) for the indicated times. Some of the cell lysates were immunoprecipitated with an antiphosphotyrosine antibody (α-PY), and the cell lysates with or without (−) the immunoprecipitation were immunoblotted with an antimouse IGF-I receptor (α-IGF-IR), an antimouse insulin receptor (α-IR), an antimouse IRS-1 (α-IRS-1), or an antimouse IRS-2 antibody (α-IRS-2). Some of the cell lysates were reciprocally immunoprecipitated with α-IGFR or α-IR and immunoblotted with α-PY. Blottings with an anti-β-actin (α-actin) were used as loading controls. Similar results were obtained in five independent experiments. The graph below shows the mean values of the band intensities of phosphorylated proteins normalized to α-actin quantified using densitometry in five independent experiments. Data are expressed as the ratio of the value at time zero. Although the data of proteins without phosphorylation are not shown in the graph, they were not significantly affected by PTH during the observation period (the ratio values were from 0.8–1.2). Data are expressed as means (*bars*) ± SEM (*error bars*) of five independent experiments. *, Significant difference from that at time zero, $P < 0.01$.

Results

Effects of PTH on cultured osteoblasts

We first examined the effects of recombinant human PTH(1–34) in the cultures of primary osteoblasts derived from mouse calvariae. IGF-I mRNA level determined by real-time RT-PCR, IGF-I protein level in the cultured medium, and ALP activity in the cell lysate were all increased about 2-fold with PTH (100 nM) treatment compared with the control cultures (Fig. 1A). A neutralizing antibody against IGF-I significantly, although not completely, suppressed the PTH stimulation of ALP activity. Furthermore, addition of a recombinant mouse IGF-1 at a concentration similar to that of endogenous IGF-I (10 mg/ml) stimulated by PTH increased the ALP activity to a level similar to that by PTH. These lines of results confirm that the PTH anabolic action is, at least partly, mediated by the IGF-I production in osteoblasts, as previously reported (8, 11, 12).

To provide some insights into signaling pathways that are involved in the PTH action on primary osteoblasts, we examined the phosphorylations of IGF-I receptor, insulin receptor, IRS-1, and IRS-2 in five independent experiments (Fig. 1B). Immunoprecipitation and immunoblotting analyses revealed that phosphorylations of IGF-I receptor and IRS-1 were clearly induced at 1 min and reached maximum at 5 min. IRS-2 was also phosphorylated by PTH, although not as strongly as IGF-I receptor and IRS-1. Insulin receptor was hardly phosphorylated by PTH. None of the protein levels of IGF-I receptor, insulin receptor, IRS-1, or IRS-2 were altered by PTH during the observation period up to 60 min, suggesting that PTH does not show transcriptional or translational regulation of these signaling molecules. These results indicate that IGF-I production followed by the activation of its intracellular signaling pathways may be related to the PTH action in osteoblasts.

Effects of PTH on bones in IRS-1−/− and IRS-2−/− mice

To learn the roles of the IRS-1 and IRS-2 in the PTH action on bone *in vivo*, we analyzed the PTH effects on the knockout mice by comparing them with those of respective WT littermates using radiological and histological analyses. Both knockout mice were healthy, with no abnormality in major organs except that *IRS-1−/−* mice alone showed about 20% shorter limbs and trunk, whereas *IRS-2−/−* mice were normal in size compared with WT littermates (19–21). The mice (10 wk old, males) were given daily sc injections of PTH (80 μg/kg) or vehicle for 4 wk, after which their femurs, tibiae, and lumbar vertebrae underwent radiological and histological analyses. As we previously reported for bone phenotypes under physiological conditions (16, 17), both knockout mice showed osteopenia when injected with vehicle: BMDs of femur, tibia, and lumbar vertebra in *IRS-1−/−* and those of femur and tibia in *IRS-2−/−* were significantly lower than respective WT littermates (Fig. 2). The PTH injection increased BMDs of these bones 10–20% in WT; however, this increase was hardly seen in the *IRS-1−/−* bones (Fig. 2A). The stimulations by PTH, on the contrary, seen in the *IRS-*

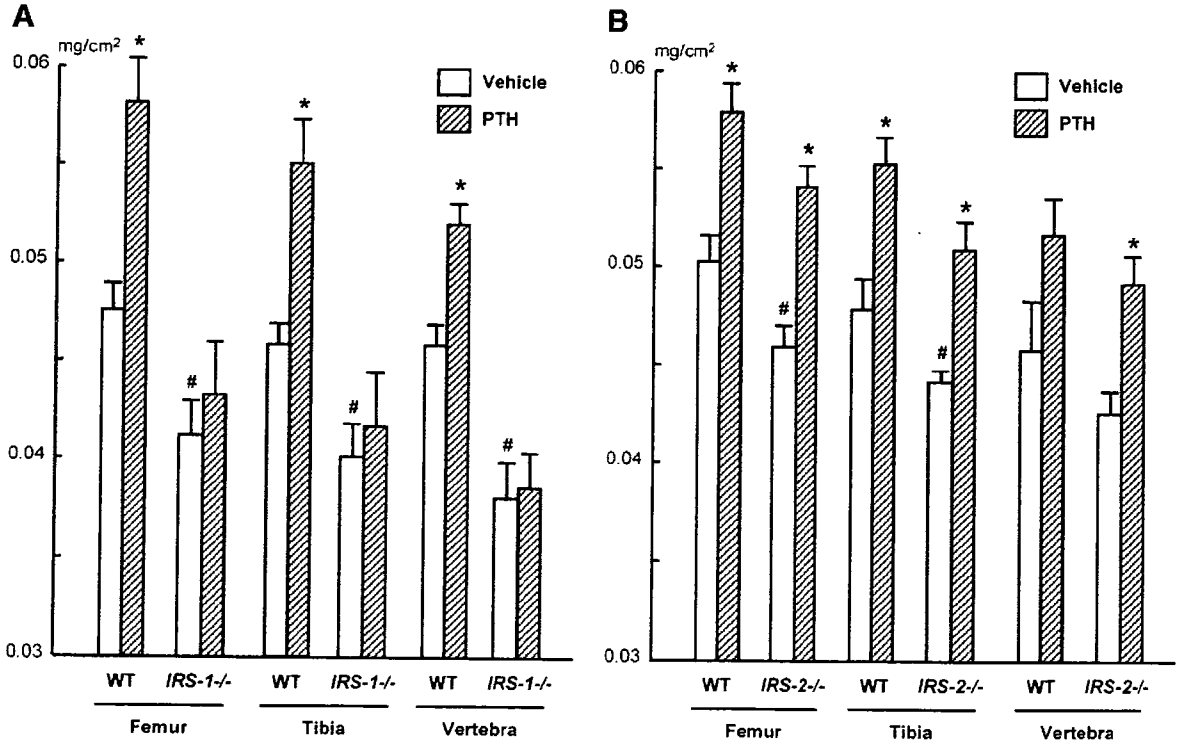

FIG. 2. Effects of PTH treatment on bone densities in *IRS-1−/−* mice (A) and *IRS-2−/−* mice (B), compared with respective WT littermates. *IRS-1−/−* mice and the littermates and *IRS-2−/−* mice and the littermates (males, 10 wk old, n = 10/group) received daily sc injections of either PTH (80 μg/kg body weight) or vehicle for 4 wk. Mice were killed; and the right femurs, tibiae, and L2–L5 vertebral bodies were excised. BMD values of the entire femurs, tibiae, and vertebral bodies were determined using dual-energy x-ray absorptiometry. Data are expressed as means (*bars*) ± SEM (*error bars*) of 10 bones per group. *, Significant effect of PTH, $P < 0.01$; #, significant difference from WT, $P < 0.01$.

2−/− bones were similar to those of the WT littermates (Fig. 2B). These results suggest that IRS-1, but not IRS-2, is needed for the bone anabolic action of PTH.

We further examined trabecular and cortical bones separately in the femurs using pQCT (Fig. 3). In trabecular bones at the distal metaphysis of femurs, both *IRS-1*−/− and *IRS-2*−/− mice showed lower bone density (Fig. 3, A and C). PTH injection increased the trabecular bone density about 60% in WT. Here again, this PTH effect was abolished by the IRS-1 deficiency but was not altered by the IRS-2 deficiency. In the cortical bones at the midshaft of the femurs, although the PTH effects on cortical thickness were milder than those on the trabecular density, this was blocked by the IRS-1 deficiency, although not by the IRS-2 deficiency (Fig. 3, B and D).

Histological features of the proximal tibiae showed decreases of trabecular bones in vehicle-treated *IRS-1*−/− and *IRS-2*−/− mice compared with the respective WT littermates (Fig. 4). After PTH treatment for 4 wk, increases of these bones were observed in *IRS-2*−/− and WT littermates to a similar extent (Fig. 4B), whereas no increase was observed in the *IRS-1*−/− trabeculae (Fig. 4A). Bone histomorphometric measurements in this area confirmed that the PTH injection augmented the bone volume (trabecular bone volume expressed as a percent of total tissue volume) of WT mice by 50–60%, with the increases of both bone formation parameters (percent of bone surface covered by cuboidal osteoclasts, and bone formation rate) and resorption parameters (percent of bone surface covered by mature osteoclasts, and percent of eroded surface), indicating a high bone turnover

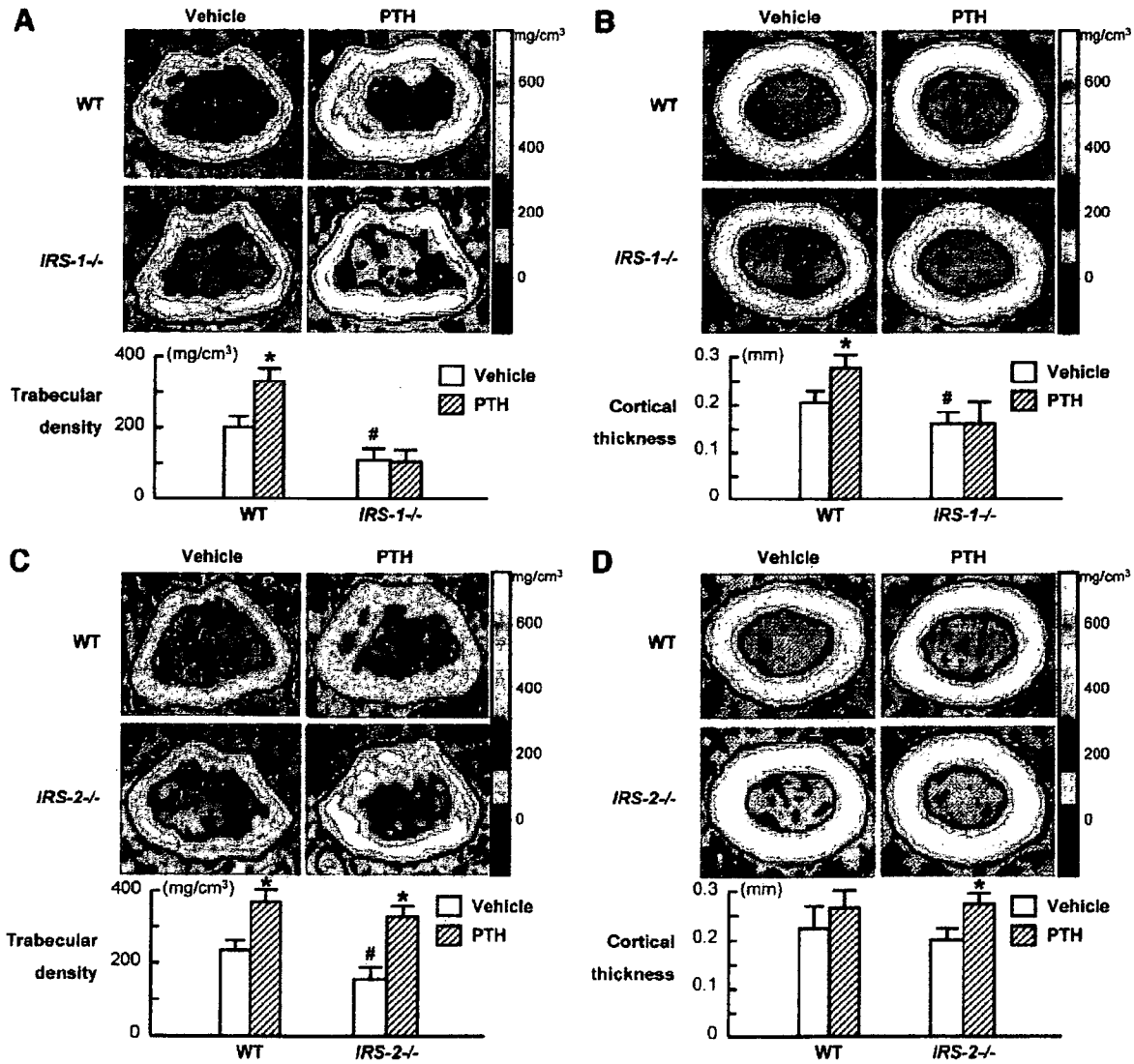

FIG. 3. Effects of PTH treatment on trabecular and cortical bones in *IRS-1*−/− mice (A and B) and *IRS-2*−/− mice (C and D), compared with respective WT littermates. After daily injections of either PTH (80 μg/kg body weight) or vehicle for 4 wk, mice were killed, and the distal metaphysis (A and C) and the middiaphysis (B and D) of the excised left femurs underwent pQCT analysis. The color gradient indicating bone density is shown in the *right bars*. The trabecular density at the metaphysis and the cortical thickness at the middiaphysis are shown in the graphs *below*. Data in all graphs are expressed as means (*bars*) ± SEMs (*error bars*) of 10 bones per group. *, Significant effect of PTH, $P < 0.01$; #, significant difference from WT, $P < 0.01$.

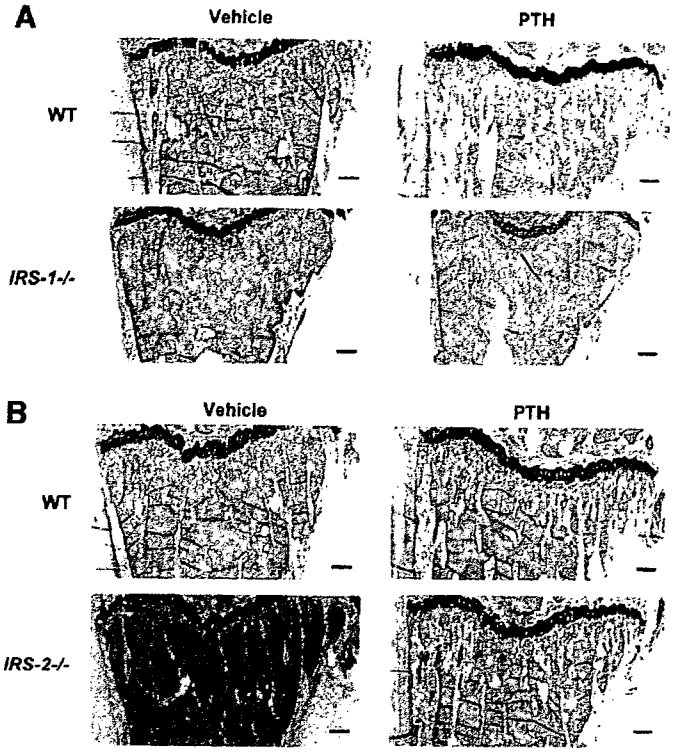

FIG. 4. Effects of PTH treatment on histological features of the proximal metaphysis of tibiae in *IRS-1−/−* mice (A) and *IRS-2−/−* mice (B), compared with respective WT littermates. After death, the left tibiae were excised, fixed, and embedded in GMA without decalcification, and the sagittal sections were stained by toluidine blue. Representative samples are shown from mice of each genotype given either PTH or vehicle. Data of histomorphometric analyses are shown in Table 1. *Bar*, 100 μm.

state (Table 1). *IRS-1−/−* and *IRS-2−/−* mice showed 30–40% lower bone volume than respective WT littermates when injected with vehicle. As we previously reported (16, 17), *IRS-1−/−* exhibited a low bone turnover, with decreases in both bone formation and resorption parameters, whereas *IRS-2−/−* mice showed an uncoupling status of bone turnover, with decreased bone formation and increased bone resorption. The PTH injection affected neither the bone volume nor the bone turnover in the *IRS-1−/−* mice; however, in the *IRS-2−/−* mice, PTH increased bone volume mainly through the up-regulation of bone formation rather than bone resorption.

Effects of PTH on blood chemistries in IRS-1−/− and IRS-2−/− mice

The serum markers osteocalcin and ALP supported the increase of bone formation by the PTH injection in WT mice (Fig. 5). Here again, these stimulations were not seen in *IRS-1−/−* mice but were maintained in *IRS-2−/−* mice. Because the serum IGF-I levels were not different between PTH- and vehicle-treated mice in all genotypes, IGF-I that is induced by PTH, as shown in Fig. 1A, seemed not to act as a systemic factor but to act locally in bone as an autocrine/paracrine factor.

Discussion

The present study demonstrated that the bone anabolic function of PTH is mediated by the activation of IGF-1R and IRS-1, but not IRS-2, as a downstream signaling of IGF-I that acts locally in bone. Although IRS-1 and IRS-2 are known to be essential for intracellular signaling of IGF-I and insulin, these two adaptor molecules have distinct biological roles and are differentially expressed in a variety of cells. Regarding glucose homeostasis, IRS-1 plays an important role in the metabolic actions of insulin, mainly in skeletal muscle and adipose tissue, whereas IRS-2 does so in the liver (22). Our previous studies revealed that only IRS-1, but not IRS-2, was expressed in the cartilage of the growth plate or the fracture callus, so that skeletal growth and fracture healing were impaired in *IRS-1−/−* mice, whereas they were normal in *IRS-2−/−* mice (21, 23). In bone, IRS-1 is expressed solely in cells of osteoblast lineage, whereas IRS-2 is expressed in cells of both osteoblast and osteoclast lineages (16, 17). As described above, our previous studies on bones of these two knockout mice disclosed that IRS-1 is important for maintaining bone turnover, and IRS-2 for maintaining predominance of anabolic function over catabolic function of osteoblasts (16, 17). In the meantime, previous and present studies have shown that PTH treatment increases bone turnover in animals and humans (24, 25). The fact that the suppression of bone turnover by IRS-1 deficiency suppressed the bone anabolic action of PTH suggests the importance of elevated turnover for the PTH function. This is consistent with the

TABLE 1. Histomorphometry of trabecular bones in proximal tibiae

	BV/TV (%)	Ob.S/BS (%)	BFR (mm^3/cm^2/year)	Oc.S/BS (%)	ES/BS (%)
WT + vehicle	9.35 ± 0.69	8.38 ± 0.80	4.96 ± 0.62	5.28 ± 1.39	6.02 ± 0.99
WT + PTH	14.23 ± 1.84[a]	12.27 ± 1.89	8.21 ± 0.83[a]	10.51 ± 1.35[a]	9.14 ± 0.51[a]
IRS-1−/− + vehicle	5.97 ± 0.62[b]	2.67 ± 1.02[b]	1.06 ± 0.29[b]	2.23 ± 0.38[b]	3.42 ± 0.59[b]
IRS-1−/− + PTH	6.25 ± 0.73	4.50 ± 0.93	1.31 ± 0.38	2.71 ± 1.03	4.14 ± 1.22
WT + vehicle	9.94 ± 0.81	8.49 ± 1.53	4.22 ± 0.29	4.90 ± 0.78	5.35 ± 0.71
WT + PTH	15.79 ± 1.60[a]	13.61 ± 2.24	9.72 ± 1.83[a]	8.84 ± 1.27[a]	9.60 ± 1.21[a]
IRS-2−/− + vehicle	6.86 ± 0.63[b]	12.93 ± 2.83	2.06 ± 0.31[b]	7.92 ± 0.69[b]	9.22 ± 1.09[b]
IRS-2−/− + PTH	16.95 ± 2.27[a]	15.71 ± 1.80	8.71 ± 0.59[a]	9.93 ± 1.43	11.42 ± 2.01

Parameters for the trabecular bone were measured in an area 1.2 mm in length from 250 μm below the growth plate at the proximal metaphysis of the tibiae in Villanueva-Goldner and calcein double-labeled sections. Data expressed as means and SEM for 10 bones per group. BV/TV, Trabecular bone volume expressed as a percentage of total tissue volume; Ob.S/BS, percentage of bone surface covered by cuboidal osteoblasts; BFR, bone formation rate; Oc.S/BS, percentage of bone surface covered by mature osteoclasts; ES/BS, percentage of eroded surface.

[a] Significant effect of PTH, $P < 0.01$.

[b] Significant difference from WT, $P < 0.01$.

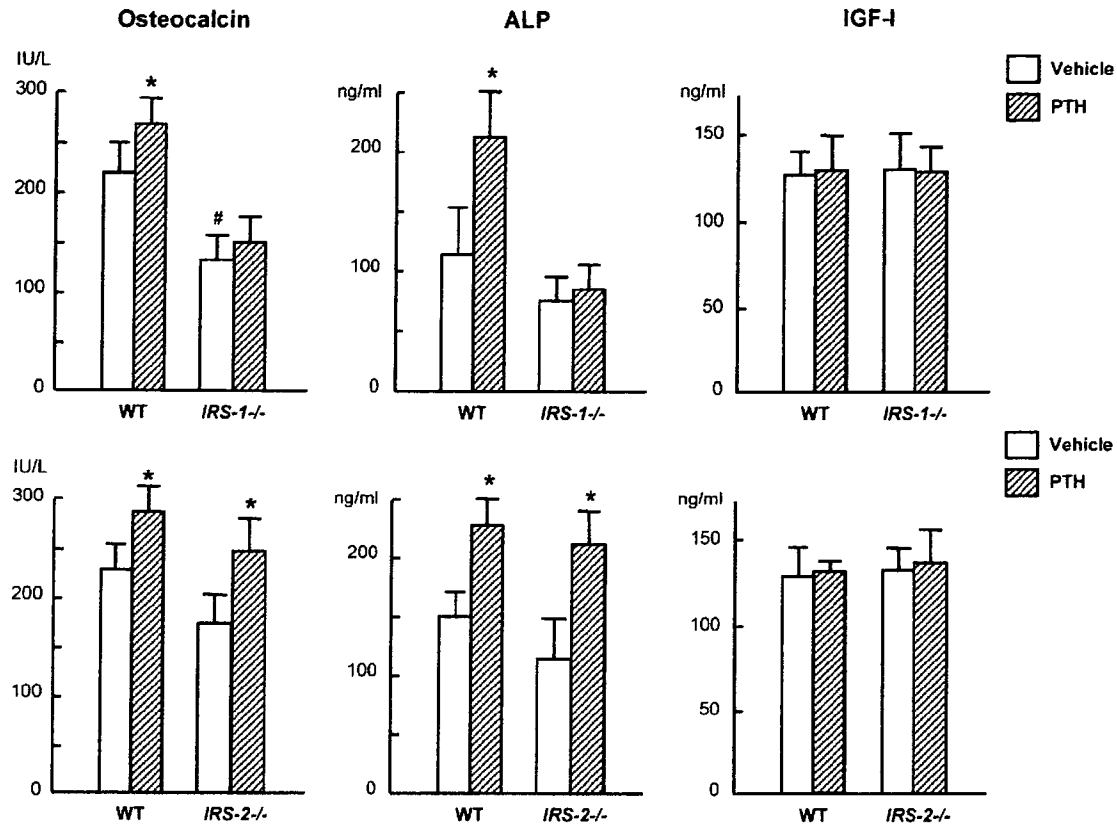

FIG. 5. Effects of PTH treatment on serum osteocalcin, ALP, and IGF-I levels in *IRS-1−/−* mice and *IRS-2−/−* mice, compared with respective WT littermates. Mice received either PTH or vehicle for 4 wk as described above, and blood samples were collected by heart puncture before death. The levels were measured as described in *Materials and Methods*. *, Significant effect of PTH, $P < 0.05$; #, significant difference from WT, $P < 0.05$.

results of clinical studies showing that the concurrent use of alendronate, a potent bisphosphonate that markedly suppresses bone turnover, reduced the bone anabolic action of PTH in male and female osteoporosis patients (26, 27).

Because it is unlikely that PTH directly activates IGF-I receptor and IRS-1, there seem to be two possible molecular mechanisms underlying the suppression of PTH action by the IRS-1 deficiency: 1) PTH induces IGF-I production, causing IGF-I receptor and IRS-1 activation; and 2) IRS-1 signaling affects the intracellular signaling lying downstream of the PTH/PTH-related protein receptor after PTH binds to it. The quick phosphorylation of IGF-I receptor and IRS-1 after PTH treatment in primary osteoblast culture in the present study (Fig. 1B) supports the former mechanism. Hormones like PTH and prostaglandin E_2 that increase cAMP synthesis and PKA activation are reported to induce the transcription of IGF-I by way of a C/EBP (CCAAT/enhancer-binding protein)-sensitive element in exon 1 of the IGF-I gene (28, 29). However, the latter possibility cannot be denied, because the inhibition of the PTH stimulation on ALP activity by a neutralizing antibody against IGF-I was not complete, but partial, in the primary osteoblast culture (Fig. 1A). In fact, IRS-1 and PTH/PPR (PTH/PTH-related protein receptor) are known to share several common signaling pathways. The main pathways lying downstream of IRS-1 are PI3K/Akt and MAPKs, which are important regulators of cell growth and differentiation. PTH has been shown to directly activate the p42/p44 MAPK by protein kinase C-dependent, but Ras-independent, signaling in rat osteoblasts (30) and to up-regulate PI3K/Akt activity, which contributes to the MAPK activation in rat enterocytes (31). In addition, both PTH and IGF-I have been shown to be involved in the activation of c-*fos* expression (32, 33) and cyclin-dependent kinase expression in osteoblasts (34, 35). These lines of evidence indicate the PTH signaling pathway may possibly be affected by the IRS-1 signaling at several points, and the absence of an IRS-1 signaling pathway may result in the failure of PTH to stimulate key target molecules necessary for its anabolic action.

Another potential explanation for the lack of PTH response in *IRS-1−/−* mice could be the impairment of proliferation or differentiation ability of osteoprogenitor cells, so that they are insensitive not only to PTH but also to other stimulations. In fact, our present and previous studies demonstrated the decreases in histomorphometric parameters and serum markers for bone formation in *IRS-1−/−* mice under physiological conditions (16). In this regard, however, our previous study has shown that proliferation and differentiation of primary calvarial cells were stimulated, responding to fibroblast growth factor-2 and bone morphogenetic protein-2, respectively, similarly to those of the WT cells, indicating that functions of *IRS-1−/−* cells are normal as long as adequate signals other than IGF-I signal were applied (16). Hence, the decreased bone formation under physiological conditions in *IRS-1−/−* mice is likely to be due to the deficit

of anabolic signaling of endogenous IGF-I. Interestingly, PTH increased the IGF-I protein level in the culture medium of primary osteoblasts (Fig. 1A) but did not affect the serum IGF-I level *in vivo* (Fig. 5), indicating the importance of local action of IGF-I as an autocrine/paracrine factor for bone formation rather than its systemic action as a hormone. This result is consistent with previous reports that disruption of IGF-I genes, specifically in liver, decreased serum IGF-I by 80% but caused no skeletal abnormality (36, 37). Because the remaining 20% IGF-I in serum is probably derived from several tissues, including bone, it is not surprising that PTH treatment did not increase circulating levels of IGF-I. The findings that PTH anabolic effects can be suppressed by an IGF-I-neutralizing antibody in osteoblast cultures in the present and previous studies (11, 12) also support the idea that the PTH-induced bone formation involves increased local production, but not increased circulating levels, of IGF-I.

The requirement of IGF-I/IRS-1 for mediating the anabolic effects of bone regulatory hormones may not be unique to PTH, because previous findings have revealed that many of the major hormones exert significant effects on IGF-I expression. GH is a well-known stimulus of IGF-I production in a variety of tissues, including bone, and exerts its effects on bone mainly through IGF-I mediation (38). Estradiol, another important regulator of skeletal metabolism, has been shown to increase IGF-I production, and IGF-I receptor-blocking antibodies inhibited the proliferative effect of estradiol in rat osteoblasts (39, 40). Similarly, other hormones with potent effects on bone, such as thyroid hormone and androgens, alter IGF-I levels in bone in a manner consistent with IGF-I playing a role in the actions of these hormones on bone (41, 42). Although these studies did not examine the involvement of IRS-1 or IRS-2 in their anabolic actions, it is possible that the IGF/IRS pathway might be a common signaling for actions of these major hormones in bone. Further understanding of the molecular mechanism by which the hormones induce IGF-I and the intracellular signaling that lies downstream of IGF-I/IRS in osteoblasts will greatly help to elucidate the complex network of bone formation under systemic regulations.

Acknowledgments

Received November 22, 2004. Accepted February 4, 2005.

Address all correspondence and requests for reprints to: Hiroshi Kawaguchi, M.D., Ph.D., Department of Sensory and Motor System Medicine, University of Tokyo, Hongo 7-3-1, Bunkyo-ku, Tokyo 113-8655, Japan. E-mail: kawaguchi-ort@h.u-tokyo.ac.jp.

This work was supported by Grants-in-Aid for Scientific Research nos. 11470301 and 12137201 from the Japanese Ministry of Education, Science, Sports, Culture and Technology.

References

1. Dempster DW, Cosman F, Parisien M, Shen V, Lindsay R 1994 Anabolic actions of parathyroid hormone on bone. Endocr Rev 15:261–280
2. Eastell R 1998 Treatment of postmenopausal osteoporosis. N Engl J Med 338:736–745
3. Neer RM, Arnaud CD, Zanchetta JR, Prince R, Gaich GA, Reginster JY, Hodsman AB, Eriksen EF, Ish-Shalom S, Genant HK, Wang O, Mitlak BH 2001 Effect of parathyroid hormone (1–34) on fractures and bone mineral density in postmenopausal women with osteoporosis. N Engl J Med 344:1434–1441
4. Rosen CJ 2003 The cellular and clinical parameters of anabolic therapy for osteoporosis. Crit Rev Eukaryot Gene Expr 13:25–38
5. Isogai Y, Akatsu T, Ishizuya T, Yamaguchi A, Hori M, Takahashi N, Suda T 1996 Parathyroid hormone regulates osteoblast differentiation positively or negatively depending on the differentiation stages. J Bone Miner Res 11:1384–1393
6. Nishida S, Yamaguchi A, Tanizawa T, Endo N, Mashiba T, Uchiyama Y, Suda T, Yoshiki S, Takahashi E 1994 Increased bone formation by intermittent parathyroid hormone administration is due to the stimulation of proliferation and differentiation of osteoprogenitor cells in bone marrow. Bone 15:717–723
7. Jilka RL, Weinstein RS, Bellido T, Roberson P, Parfitt AM, Manolagas SC 1999 Increased bone formation by prevention of osteoblast apoptosis with parathyroid hormone. J Clin Invest 104:439–446
8. McCarthy TL, Centrella M, Canalis E 1989 Parathyroid hormone enhances the transcript and polypeptide levels of insulin-like growth factor I in osteoblast-enriched cultures from fetal rat bone. Endocrinology 124:1247–1253
9. Watson P, Lazowski D, Han V, Fraher L, Steer B, Hodsman A 1995 Parathyroid hormone restores bone mass and enhances osteoblast insulin-like growth factor I gene expression in ovariectomized rats. Bone 16:357–365
10. Canalis E 1993 Insulin like growth factors and the local regulation of bone formation. Bone 14:273–276
11. Canalis E, Centrella M, Burch W, McCarthy TL 1989 Insulin-like growth factor I mediates selective anabolic effects of parathyroid hormone in bone cultures. J Clin Invest 83:60–65
12. Ishizuya T, Yokose S, Hori M, Noda T, Suda T, Yoshiki S, Yamaguchi A 1997 Parathyroid hormone exerts disparate effects on osteoblast differentiation depending on exposure time in rat osteoblastic cells. J Clin Invest 99:2961–2970
13. Miyakoshi N, Kasukawa Y, Linkhart TA, Baylink DJ, Mohan S 2001 Evidence that anabolic effects of PTH on bone require IGF-I in growing mice. Endocrinology 142:4349–4356
14. Bikle DD, Sakata T, Leary C, Elalieh H, Ginzinger D, Rosen CJ, Beamer W, Majumdar S, Halloran BP 2002 Insulin-like growth factor I is required for the anabolic actions of parathyroid hormone on mouse bone. J Bone Miner Res 17:1570–1578
15. Kadowaki T, Tobe K, Honda-Yamamoto R, Tamemoto H, Kaburagi Y, Momomura K, Ueki K, Takahashi Y, Yamauchi T, Akanuma Y, Yazaki Y 1996 Signal transduction mechanism of insulin and insulin-like growth factor-1. Endocr J 43:S33–S41
16. Ogata N, Chikazu D, Kubota N, Terauchi Y, Tobe T, Azuma Y, Ohta T, Kadowaki T, Nakamura K, Kawaguchi H 2000 Insulin receptor substrate-1 in osteoblast is indispensable for maintaining bone turnover. J Clin Invest 105:935–943
17. Akune T, Hoshi K, Kubota Y, Terauchi K, Tobe Y, Azuma T, Ohta T, Nakamura K, Kawaguchi H 2002 Insulin receptor substrate-2 maintains predominance of anabolic function over catabolic function of osteoblasts. J Cell Biol 159:147–156
18. Parfitt AM, Drezner MK, Glorieux FH, Kanis JA, Malluche H, Meunier PJ, Ott SM, Recker RR 1987 Bone histomorphometry: standardization of nomenclature, symbols, and units. Report of the ASBMR Histomorphometry Nomenclature Committee. J Bone Miner Res 2:595–610
19. Tamemoto H, Kadowaki T, Tobe K, Yagi T, Sakura H, Hayakawa T, Terauchi Y, Ueki K, Kaburagi Y, Satoh S, Nagai R, Yazaki T 1994 Insulin resistance and growth retardation in mice lacking insulin receptor substrate-1. Nature 372:182–186
20. Kubota N, Tobe K, Terauchi Y, Eto K, Yamauchi T, Suzuki R, Tsubamoto Y, Komeda K, Nakano R, Miki H, Satoh S, Sekihara H, Sciacchitano S, Lesniak M, Aizawa S, Nagai R, Kimura S, Akanuma Y, Taylor SI, Kadowaki T 2000 Disruption of insulin receptor substrate 2 causes type 2 diabetes because of liver insulin resistance and lack of compensatory β-cell hyperplasia. Diabetes 49:1880–1889
21. Hoshi K, Ogata N, Shimoaka T, Terauchi Y, Kadowaki T, Kenmotsu S, Chung UI, Ozawa H, Nakamura K, Kawaguchi H 2004 Deficiency of insulin receptor substrate-1 impairs skeletal growth through early closure of epiphyseal cartilage. J Bone Miner Res 19:214–223
22. Bruning JC, Winnay J, Cheatham B, Kahn CR 1997 Differential signaling by insulin receptor substrate 1 (IRS-1) and IRS-2 in IRS-1-deficient cells. Mol Cell Biol 17:1513–1521
23. Shimoaka T, Kamekura S, Chikuda H, Hoshi K, Chung UI, Akune T, Maruyama Z, Komori T, Matsumoto M, Ogawa W, Terauchi Y, Kadowaki T, Nakamura K, Kawaguchi H 2004 Impairment of bone healing by insulin receptor substrate-1 deficiency. J Biol Chem 279:15314–15322
24. Sato M, Westmore M, Ma YL, Schmidt A, Zeng QQ, Glass EV, Vahle J, Brommage R, Jerome CP, Turner CH 2004 Teriparatide [PTH(1–34)] strengthens the proximal femur of ovariectomized nonhuman primates despite increasing porosity. J Bone Miner Res 19:623–629
25. Dempster DW, Cosman F, Kurland ES, Zhou H, Nieves J, Woelfert L, Shane E, Plavetic K, Muller R, Bilezikian J, Lindsay R 2001 Effects of daily treatment with parathyroid hormone on bone microarchitecture and turnover in patients with osteoporosis: a paired biopsy study. J Bone Miner Res 16:1846–1853
26. Black DM, Greenspan SL, Ensrud KE, Palermo L, McGowan JA, Lang TF, Garnero P, Bouxsein ML, Bilezikian JP, Rosen CJ; PTH Study Investigators

2003 The effects of parathyroid hormone and alendronate alone or in combination in postmenopausal osteoporosis. N Engl J Med 349:1207–1215
27. **Finkelstein JS, Hayes A, Hunzelman JL, Wyland JJ, Lee H, Neer RM** 2003 The effects of parathyroid hormone, alendronate, or both in men with osteoporosis. N Engl J Med 349:1216–1226
28. **Umayahara Y, Billiard J, Ji C, Centrella M, McCarthy TL, Rotwein P** 1999 CCAAT/enhancer-binding protein ô is a critical regulator of insulin-like growth factor-I gene transcription in osteoblasts. J Biol Chem 274:10609–10617
29. **Chang W, Rewari A, Centrella M, McCarthy TL** 2004 Fos-related antigen 2 controls protein kinase A-induced CCAAT/enhancer-binding protein β expression in osteoblasts. J Biol Chem 279:42438–42444
30. **Swarthout JT, Doggett TA, Lemker JL, Partridge NC** 2001 Stimulation of extracellular signal-regulated kinases and proliferation in rat osteoblastic cells by parathyroid hormone is protein kinase C-dependent. J Biol Chem 276: 7586–7592
31. **Gentili C, Morelli S, Russo De Boland A** 2002 Involvement of PI3-kinase and its association with c-Src in PTH-stimulated rat enterocytes. J Cell Biochem 86:773–783
32. **Lee K, Deeds JD, Chiba S, Un-No M, Bond AT, Segre GV** 1994 Parathyroid hormone induces sequential c-*fos* expression in bone cells in vivo: *in situ* localization of its receptor and c-*fos* messenger ribonucleic acids. Endocrinology 134:441–450
33. **Merriman HL, La Tour D, Linkhart TA, Mohan S, Baylink DJ, Strong DD** 1990 Insulin-like growth factor-I and insulin-like growth factor-II induce c-*fos* in mouse osteoblastic cells. Calcif Tissue Int 46:258–262
34. **Onishi T, Zhang W, Cao X, Hruska K** 1997 The mitogenic effect of parathyroid hormone is associated with E2F-dependent activation of cyclin-dependent kinase 1 (cdc2) in osteoblast precursors. J Bone Miner Res 12:1596–1605
35. **Furlanetto RW, Harwell SE, Frick KK** 1994 Insulin-like growth factor-I induces cyclin-D1 expression in MG63 human osteosarcoma cells *in vitro*. Mol Endocrinol 8:510–517
36. **Yakar S, Liu JL, Stannard B** 1999 Normal growth and development in the absence of hepatic insulin-like growth factor I. Proc Natl Acad Sci USA 96: 7324–7329
37. **Sjogren K, Liu JL, Blad K** 1999 Liver-derived insulin-like growth factor I (IGF-I) is the principal source of IGF-I in blood but is not required for postnatal body growth in mice. Proc Natl Acad Sci USA 96:7088–7092
38. **Ohlsson C, Bengtsson BA, Isaksson OG, Andreassen TT, Slootweg MC** 1998 Growth hormone and bone. Endocr Rev 19:55–79
39. **Gray TK, Mohan S, Linkhart TA, Baylink DJ** 1989 Estradiol stimulates *in vitro* the secretion of insulin-like growth factors by the clonal osteoblastic cell line, UMR106. Biochem Biophys Res Commun 158:407–412
40. **Cheng M, Zaman G, Rawlinson SC, Mohan S, Baylink DJ, Lanyon LE** 1999 Mechanical strain stimulates ROS cell proliferation through IGF-II and estrogen through IGF-I. J Bone Miner Res 14:1742–1750
41. **Gori F, Hofbauer LC, Conover CA, Khosla S** 1999 Effects of androgens on the insulin-like growth factor system in an androgen-responsive human osteoblastic cell line. Endocrinology 140:5579–5586
42. **Huang BK, Golden LA, Tarjan G, Madison LD, Stern PH** 2000 Insulin-like growth factor I production is essential for anabolic effects of thyroid hormone in osteoblasts. J Bone Miner Res 15:188–197

Endocrinology **is published monthly by The Endocrine Society (http://www.endo-society.org), the foremost professional society serving the endocrine community.**

Available online at www.sciencedirect.com
SCIENCE DIRECT
ELSEVIER
Biochemical and Biophysical Research Communications 338 (2005) 872–879
BBRC
www.elsevier.com/locate/ybbrc

Mechanism of osteogenic induction by FK506 via BMP/Smad pathways

Fumitaka Kugimiya [a,b], Fumiko Yano [a], Shinsuke Ohba [a], Kazuyo Igawa [a], Kozo Nakamura [b], Hiroshi Kawaguchi [b], Ung-il Chung [a,*]

[a] *Division of Tissue Engineering, Faculty of Medicine, University of Tokyo, Hongo 7-3-1, Bunkyo, Tokyo 113-8655, Japan*
[b] *Division of Sensory and Motor System Medicine, Faculty of Medicine, University of Tokyo, Hongo 7-3-1, Bunkyo, Tokyo 113-8655, Japan*

Received 1 October 2005
Available online 14 October 2005

Abstract

FK506 is an immunosuppressant that exerts effects by binding to FK506-binding protein 12 (FKBP12). Recently, FK506 has also been reported to promote osteogenic differentiation when administered locally or in vitro in combination with bone morphogenetic proteins (BMPs), although the underlying mechanism remains unclarified. The present study initially showed that FK506 alone at a higher concentration (1 μM) induced osteogenic differentiation of mesenchymal cell lines, which was suppressed by adenoviral introduction of Smad6. FK506 rapidly activates the BMP-dependent Smads in the absence of BMPs, and the activation was blocked by Smad6. Overexpression of FKBP12, which was reported to block the ligand-independent activation of BMP type I receptor A (BMPRIA), suppressed Smad signaling induced by FK506, but not that induced by BMP2. BMPRIA and FKBP12 bound to each other, and this binding was suppressed by FK506. These data suggest that FK506 promotes osteogenic differentiation by activating BMP receptors through interacting with FKBP12.

Keywords: FK506; BMP; Smad; FKBP12; Osteogenic differentiation; Osteoblast

FK506 is an immunosuppressive agent with an increasing number of clinical applications [1–4]. FK506 exerts its immunosuppressive effects by binding to the FK506-binding protein 12 (FKBP12) [5]. The complex of FK506 and FKBP12 inactivates calcineurin, resulting in the inhibition of the cytokine expression including interleukin-2, interleukin-3, and γ-interferon in T cells and the consequent immunosuppression [6]. In addition to its immunosuppressive activity, FK506 has been shown to exert a variety of actions on bone metabolism. When administered systemically, FK506 causes osteopenia in mice, rats, and humans [7–11]. When administered locally or in vitro in combination with bone morphogenetic proteins (BMPs), FK506 promotes osteogenic differentiation [12–14].

BMPs are members of secreted signaling proteins that belong to the transforming growth factor-β (TGF-β) superfamily. BMPs were originally identified as molecules that induced ectopic bone formation when implanted into the rodent muscle [15,16]. In accordance with such in vivo effects, the BMPs have been shown to regulate osteogenic differentiation in vitro [17]. They bind to a characteristic pair of transmembrane serine/threonine kinase receptors, BMP type I and type II receptors (BMPRI and BMPRII). They first bind to the BMPRII, which phosphorylates the GS region of the BMPRI [18]. The activated BMPRI subsequently recruits and phosphorylates Smad1, Smad5, and Smad8 (the BMP-dependent Smads) through the GS region. The BMP-dependent Smads then physically associate with Smad4, translocate into the nucleus, and activate the target genes. Smad6 blocks BMP signaling by inhibiting the phosphorylation of the BMP-dependent Smads by the BMPRI. FKBP12 has been reported to block the ligand-independent activation of the BMPRI [19], but whether FKBP12 mediates the interactions of BMP signaling and FK506 remains unknown. The current study investigated

* Corresponding author. Fax: +81 3 3818 4082.
E-mail address: uichung-tky@umin.ac.jp (U. Chung).

0006-291X/$ - see front matter © 2005 Elsevier Inc. All rights reserved.
doi:10.1016/j.bbrc.2005.10.024

the regulation and the mechanism of action of FK506 on osteogenic differentiation of mesenchymal cell lines using the in vitro culture systems.

Materials and methods

In vitro osteogenic differentiation assay. MLB13MYC clone 17 (C17), a limb bud-derived cell line, which differentiates into osteoblasts upon treatment with BMP signaling [20], was a generous gift from V. Rosen (Harvard University, MA). C2C12, a mouse myoblastic cell line, which differentiates into osteoblasts upon treatment with BMP signaling [21], was obtained from the Riken Cell Bank (Tsukuba, Japan). These cells were maintained in high glucose Dulbecco's modified Eagle's medium (DMEM, Sigma–Aldrich, St. Louis, MO) containing 10% fetal bovine serum (FBS) (Sigma–Aldrich) and 1% penicillin/streptomycin (Sigma–Aldrich). For the alkaline phosphatase (ALP) staining, the cells were fixed in 70% ETOH and stained for 10 min with a solution containing 0.01% naphthol AS-MX phosphate disodium salt (Sigma–Aldrich), 1% *N,N*-dimethylformamide (Wako Pure Chemicals Industry Tokyo), and 0.06% fast blue BB (Sigma–Aldrich). FK506, cyclosporin A (CsA), recombinant human BMP2 (rhBMP2), and Noggin were purchased from Sigma–Aldrich.

Real-time RT-PCR. The total RNA was extracted using an ISOGEN Kit (Wako) and an RNeasy Mini Kit (QIAGEN, Hilden, Germany), and treated with DNaseI (QIAGEN), according to the manufacturer's instructions. One microgram of RNA was reverse-transcribed using a Takara RNA PCR Kit (AMV) ver.2.1 (Takara, Shiga, Japan) to generate the single-stranded cDNA. PCR was performed using the ABI Prism 7000 Sequence Detection System (Applied Biosystems, Foster-city, CA). Each PCR consisted of 1XQuantiTect SYBR Green PCR Master Mix (QIAGEN), 0.3 μM specific primers, and 500 ng DNA. The mRNA copy number of a specific gene in the total RNA was calculated using a standard curve generated with serially diluted plasmids containing PCR amplicon sequences and normalized to the human or rodent total RNA (Applied Biosystems) with mouse actin as the internal control. The standard plasmids were synthesized using a TOPO TA Cloning Kit (Invitrogen, Carlsbad, CA), according to the manufacturer's instruction. All reactions were run in triplicate. The primer sequences are available upon request.

Preparation of adenoviruses and plasmids. Adenoviruses expressing LacZ and Smad6 were generous gifts from K. Miyazono (The University of Tokyo, Tokyo, Japan). Adenoviruses were amplified in HEK293 cells and purified using an AdenoX Virus Purification Kit (Clontech, Palo Alto, CA). Viral titers were determined by the end-point dilution assay. Plasmids expressing the HA-tagged BMP type I receptor A (HA-BMPRIA) and Flag-tagged FKBP12 (Flag-FKBP12), and the luciferase reporter construct responding to BMP-dependent Smad signaling (12xGCCG-luc) were generous gifts from K. Miyazono.

Luciferase assay. The human hepatoma cell line HuH-7 was obtained from the Riken Cell Bank. HuH7 cells were plated onto 24-well plates and then transfected with 0.1 μg of the reporter plasmid construct alone or in combination with the plasmid expressing HA-BMPRIA and Flag-FKBP12 for 1 day, then treated with FK506 (0.1 or 1 μM) or rhBMP2 (200 ng/ml) and cultured for 2 days. The luciferase assay was performed 48 h after transfection using a PicaGene Dual SeaPansy Luminescence Kit (Toyo Ink, Tokyo, Japan) and the Lumat LB 9507 (Berthold Technologies GmbH, KG, Wildbad, Germany). The level of luciferase activity was normalized to the level of the *Renilla* luciferase activity. All data were expressed as means ± SE ($n = 6$).

Immunoblot and immunoprecipitation assay. The cells were washed twice with ice-cold PBS, and the proteins were extracted using an M-PER Kit (Pierce Chemical, Rockford, IL) according to the manufacturer's instructions. The protein concentrations of the cell lysates were measured using a Protein Assay Kit II (Bio-Rad, Hercules, CA). For the immunoblot analysis, the lysates were fractionated by SDS–PAGE with 4–20% Tris–glycine gradient gel or 18% Tris–glycine gel (Invitrogen) and transferred onto nitrocellulose membranes (Bio-Rad). After being blocked with 6% milk/TBS-T, the membranes were incubated with the anti-Smad1 mouse monoclonal antibody (1:1000; Cell Signaling Technology, Beverly MA), anti-phospho-Smad 1/5/8 (1:1000; Cell Signaling Technology), anti-HA mouse monoclonal antibody (1:1000; Santa Cruz Biolaboratories, Santa Cruz, CA), or anti-Flag rabbit antibody (1:1000; Sigma–Aldrich). The secondary antibodies, i.e., HRP-conjugated goat anti-mouse IgG (Promega, Madison, WI) and goat anti-rabbit IgG (Promega), were used at dilutions of 1:10,000. The immunoreactive bands were visualized using an ECL Plus Kit (Amersham, Arlington Heights, IL) according to the manufacturer's instructions.

For immunoprecipitation, 293 cell extracts were incubated with 5 μg of anti-HA and anti-Flag antibodies at 4 °C overnight. The immune complexes were recovered with protein G–Sepharose (Sephadex G-50 Fine; Amersham Life Sciences), subjected to SDS–PAGE, and then transferred onto nitrocellulose membranes. Immunoblotting was performed as already described.

Statistical analysis. Means of groups were compared by ANOVA, and the significance of differences was determined by post hoc testing using Bonferroni's method.

Results

Induction of osteogenic differentiation by FK506

To clarify the effect of FK506 on osteogenic differentiation, we treated the limb bud-derived cell line C17 with FK506 at concentrations ranging from 0.01 to 10 μM. This cell line has been shown to rapidly undergo osteogenic differentiation upon treatment with BMP signaling [20]. Consistent with the report by Tang et al. [12], the treatment with FK506 at 0.1 μM for 3 days induced the ALP activity determined by the ALP staining, but not the osteocalcin mRNA expression determined by the real-time RT-PCR analysis (Figs. 1A and B). When we treated the cells with FK506 at 1 μM, however, both the ALP activity and osteocalcin expression were induced. When the cells were treated with FK506 at 10 μM, neither the ALP activity nor osteocalcin expression was induced (data not shown), probably due to the toxic effect of the drug. In contrast, CsA, an immunosuppressive drug, which also inhibits calcineurin, did not increase the ALP activity or osteocalcin expression at the concentrations tested (Figs. 1A and B). The induction of the ALP activity and osteocalcin expression by FK506 (1 μM) was also seen in C2C12 cells (Figs. 1C and D). These data suggest that FK506 alone is able to induce osteogenic differentiation and that the effect of FK506 on osteogenic differentiation is not dependent on calcineurin signaling.

Interactions of FK506 and BMP signaling during osteogenic differentiation

Since FK506 has been reported to enhance BMP signaling [12], we investigated the interactions of FK506 and BMP signaling. We treated C17 cells with rhBMP2 at various concentrations in the presence or absence of FK506 (1 μM). The ALP activity induced by rhBMP2 was dose-dependent and reached the maximal intensity at 500 ng/ml (Fig. 2A). The ALP activity induced by FK506 alone was more intense than that induced by rhBMP2 at

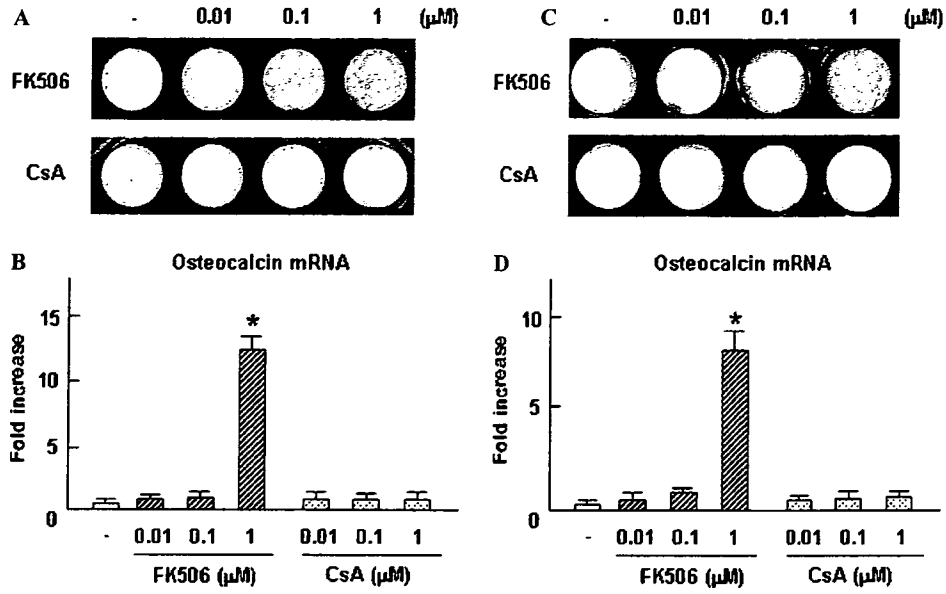

Fig. 1. Induction of osteogenic differentiation by FK506. (A) ALP staining of C17 cells cultured for 3 days in the presence or absence of FK506 or Cyclosporin A (CsA) at various concentrations. (B) Real-time RT-PCR analysis of osteocalcin expression using total RNA isolated from the above-mentioned C17 cells. Data are expressed as means ± SEM of six wells per group. $^*P < 0.01$ vs. no treatment. (C) ALP staining of C2C12 cells cultured for 3 days in the presence or absence of FK506 or CsA at various concentrations. (D) Real-time RT-PCR analysis of osteocalcin expression using total RNA isolated from the above-mentioned C2C12 cells. Data are expressed as means ± SEM of six wells per group. $^*P < 0.01$ vs. no treatment.

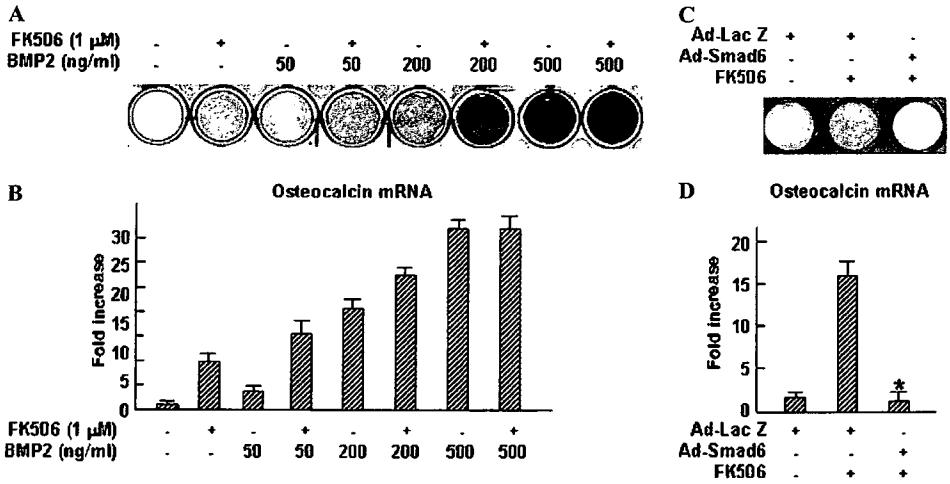

Fig. 2. Interactions of FK506 and BMP signaling in osteogenic differentiation. (A) ALP staining of C17 cells cultured for 3 days in the presence of BMP2 at various concentrations with or without FK506 (1 μM). (B) Real-time RT-PCR analysis of osteocalcin expression using total RNA isolated from the above-mentioned C17 cells. Data are expressed as means ± SEM of six wells per group. $^*P < 0.01$ vs. no treatment. (C) ALP staining of C17 cells infected with an adenovirus expressing LacZ (Ad-LacZ) or an adenovirus expressing Smad6 (Ad-Smad6) for 2 days, and then cultured for 3 days in the presence or absence of FK506 (1 μM). (D) Real-time RT-PCR analysis of osteocalcin expression using total RNA isolated from the above-mentioned C17 cells. Data are expressed as means ± SEM of six wells per group. $^*P < 0.01$ vs. Ad-LacZ+FK506.

50 ng/ml, but less intense than that induced by rhBMP2 at 200 ng/ml. The addition of FK506 to rhBMP2 increased the intensity of the staining by approximately the amount induced by FK506 alone. The real-time RT-PCR analysis of the osteocalcin expression concurred with these data (Fig. 2B). These results suggest that the effect of FK506 on BMP signaling is additive rather than synergistic.

To further investigate whether the osteogenic effect of FK506 required BMP signaling, C17 cells were infected with an adenovirus expressing Smad6 (Ad-Smad6), an inhibitor of BMP signaling, for 2 days and cultured for 3 days in the presence of FK506. The ALP staining and real-time PCR analysis of the osteocalcin expression revealed that the treatment with Ad-Smad6 suppressed

osteogenic differentiation induced by FK506 (Figs. 2C and D).

Activation of BMP-dependent Smads by FK506

Next, we investigated whether FK506 exerted its osteogenic effect by activating the BMP-dependent Smads. The 12xGCCG-luc reporter construct contains the DNA binding site of the BMP-dependent Smads and expresses luciferase in response to BMP signaling [22]. When a human hepatoma cell line HuH-7 was transfected with the 12xGCCG-luc reporter construct in combination with FK506 (0.1 or 1 μM) or rhBMP2 (200 ng/ml), FK506 (1 μM) induced the promoter activity, which was about 60% as strong as that induced by rhBMP2 (Fig. 3A). The transcription of the inhibitor of differentiation-1 (ID-1) has been reported to be dependent on BMP signaling, and its promoter contains a functional DNA binding site for BMP-dependent Smads [23]. When C17 cells were treated with FK506 (1 μM) for 30 min to 5 h, the real-time RT-PCR analysis revealed that FK506 started inducing the ID-1 mRNA expression within a period as short as 30 min, with the expression reaching its peak at 3 h (Fig. 3B). The immunoblot analysis showed that the treatment of C17 cells with FK506 (1 μM) induced the phosphorylation of the BMP-dependent Smads (Fig. 3C). The induction started within a period as short as 30 min, reaching its peak at 1 h and was sustained for up to 5 h.

The results so far suggest that FK506 activates the BMP-dependent Smads in a short period, probably without involving the transcription or translation of the new genes. There are two possible molecular mechanisms. First, FK506 may activate the BMP receptor or the BMP-dependent Smads. Second, FK506 may amplify the action of the existing BMPs. These experiments were carried out in the presence of fetal bovine serum that might contain an undetermined amount of BMPs [24], thus making it difficult to distinguish between these two possibilities. To overcome this problem, C17 cells were cultured in serum-free DMEM with FK506 (1 μM) or rhBMP2 (200 ng/ml) in the presence or absence of simultaneous treatment with Noggin (1000 ng/ml), a potent BMP antagonist. The immunoblot analysis revealed that FK506 induced the phosphorylation of the BMP-dependent Smads in serum-free medium, and that Noggin blocked the

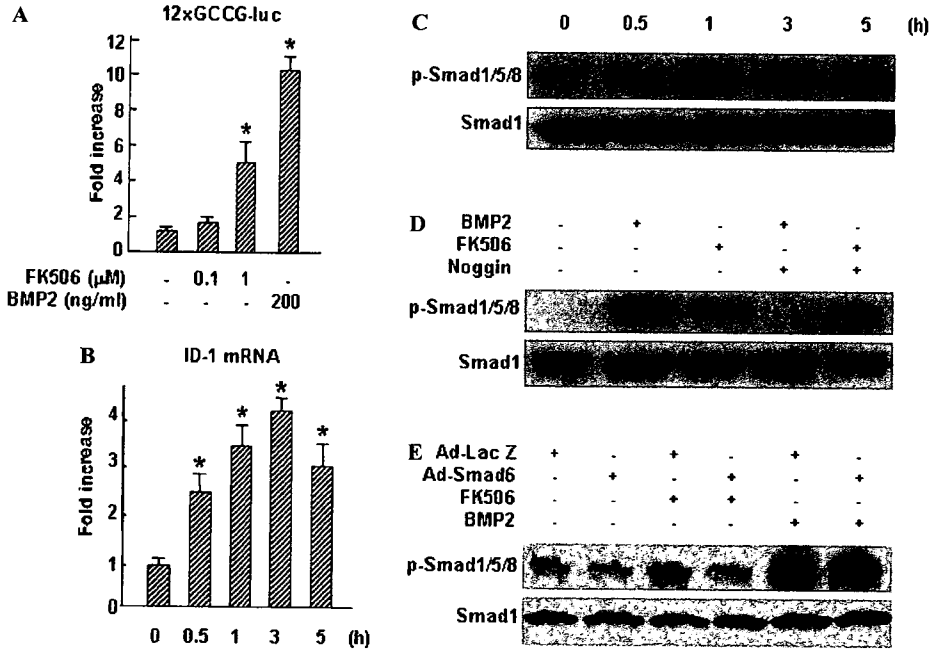

Fig. 3. Activation of the BMP-dependent Smads by FK506. (A) Luciferase reporter analysis of the effect of FK506 on the BMP-dependent promoter activity. Whole cell lysates were collected from HuH-7 cells transfected with the 12xGCCG-luc reporter plasmid construct alone or in combination with FK506 or rhBMP2 and cultured for 2 days. Data are expressed as means ± SEM of six wells per group. $*P < 0.01$ vs. the reporter plasmid alone. (B) Time course of ID-1 expression determined by real-time RT-PCR using total RNA isolated from C17 cells treated with FK506 (1 μM) for 0.5, 1, 3, and 5 h. Data are expressed as means ± SEM of six wells per group. $*P < 0.01$ vs. time 0. (C) Time course of induction of Smad1/5/8 phosphorylation by FK506 determined by immunoblot analysis using anti-phospho-Smad1/5/8 antibody (upper panel). Whole cell extracts were collected from C17 cells treated with FK506 (1 μM) for 0, 0.5, 1, 2, 3, 4, and 5 h. The lower panel shows expression of Smad1 to demonstrate normalized loading of proteins. (D) The effect of Noggin on FK506-induced phosphorylation of Smad 1/5/8 determined by immunoblot analysis using an anti-phospho-Smad1/5/8 antibody (upper panels). Whole cell extracts were collected from C17 cells cultured in serum-free DMEM with FK506 (1 μM) or rhBMP2 (200 ng/ml) in the presence or absence of simultaneous treatment with Noggin (1000 ng/ml). The lower panel shows expression of Smad1 to demonstrate normalized loading of proteins. (E) The effect of Smad6 on FK506-induced phosphorylation of Smad 1/5/8 determined by immunoblot analysis using an anti-phospho-Smad1/5/8 antibody (upper panels). Whole cell extracts were collected from C17 cells infected with Ad-Smad6 for 2 days and cultured in the presence of FK506 (1 μM) or rhBMP2 (200 ng/ml) for 1 h. The lower panel shows expression of Smad1 to demonstrate normalized loading of proteins.

phosphorylation of these Smads induced by rhBMP2, but not that induced by FK506. To determine whether FK506 phosphorylates the BMP-dependent Smads through activating the BMP receptors, the effect of Smad6, which binds and inactivates the BMP receptors, on the phosphorylation was investigated. Immunoblot analysis using an anti-phospho Smad1/5/8 antibody revealed that the phosphorylation of Smads by FK506 was suppressed by the adenoviral expression of Smad6 (Fig. 3E). Taken together, these results strongly suggest that FK506 activates the BMP receptors.

Interactions of FK506, the BMP receptors, and FKBP12

In the meantime, FKBP12 has been reported to block the ligand-independent activation of the TGF-β type I receptor, which is homologous to the BMPRI, by binding to the two amino acids of the GS region [25]. FKBP12 has also been reported to block the ligand-independent activation of the BMPRIA [19]. Since the GS region is well conserved between the TGF-β type I receptor and the BMPRI, FK506 may activate the BMPRI by dissociating them from FKBP12. The luciferase reporter analysis revealed that the BMP-dependent promoter activity induced by FK506 was suppressed by the overexpression of FKBP12 (Fig. 4A). The immunoprecipitation and immunoblot analyses revealed that the BMPRIA and FKBP12 bound to each other when they were overexpressed in 293 cells, and this binding was attenuated by treatment with FK506 (Fig. 4B).

To clarify the role of FKBP12 in BMP-induced Smad signaling, the effect of FKBP12 on the BMP-induced Smad phosphorylation was investigated. Immunoblot analysis revealed that overexpression of FKBP12 at various concentrations did not affect the BMP-induced phosphorylation of Smad1/5/8 (Fig. 4C). These data suggest that FKBP12 does not inhibit the BMP-activated BMPRI. Next, we examined the effect of FK506 on the BMP-induced Smad phosphorylation, because FK506 and BMP additively promoted osteogenic differentiation. The immunoblot analysis revealed that BMP-induced phosphorylation of Smad1/5/8 was increased by addition of FK506 in a dose-dependent manner (Fig. 4D).

Discussion

In the current paper, we demonstrate that FK506 alone at a higher concentration induces the osteocalcin expression in the mesenchymal cell lines, while CsA does not;

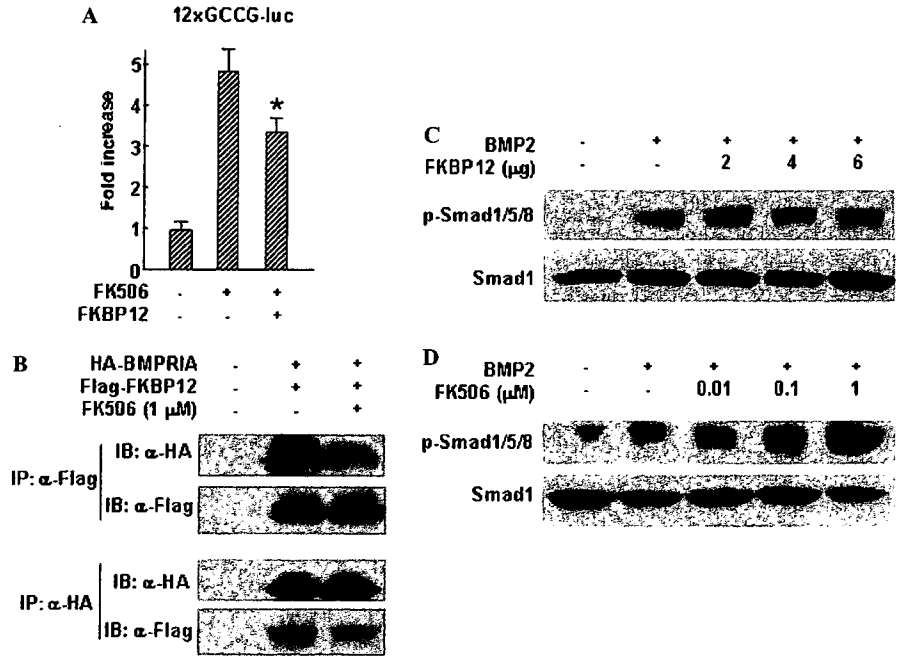

Fig. 4. Interactions of FK506, BMPRI, and FKBP12. (A) Luciferase reporter analysis of the effect of FKBP12 on the FK506-activated BMP-dependent promoter activity. Whole cell lysates were collected from HuH-7 cells transfected with the 12xGCCG-luc reporter plasmid construct alone or in combination with the plasmid expressing HA-BMPRIA and Flag-FKBP12 for 1 day, and then treated with FK506 (1 μM) and cultured for 2 days. Data are expressed as means ± SEM of six wells per group. $^*P < 0.01$ vs. FK506 alone. (B) Physical association of BMPRIA and FKBP12 determined by the immunoprecipitation (IP) and immunoblot (IB) analysis using anti-HA and anti-Flag antibodies. Cell extracts were prepared from 293 cells transfected with or without plasmids expressing HA-BMPRIA and Flag-FKBP12 in the absence or presence of FK506 (1 μM). (C) The effect of FKBP12 on BMP-induced phosphorylation of Smad 1/5/8 determined by immunoblot analysis using an anti-phospho-Smad1/5/8 antibody (upper panel). Whole cell extracts were collected from C17 cells transfected in 6-cm dishes with the plasmid expressing FKBP12 (2, 4 or 6 μg) with rhBMP2 (100 ng/ml). The lower panel shows expression of Smad1 to demonstrate normalized loading of proteins. (D) The effect of FK506 on BMP-induced phosphorylation of Smad 1/5/8 determined by immunoblot analysis using an anti-phospho-Smad1/5/8 antibody (upper panel). Whole cell extracts were collected from C17 cells treated with rhBMP2 (100 ng/ml) in the presence or absence of FK506 at concentrations ranging from 0.01 to 1 μM. The lower panel shows expression of Smad1 to demonstrate normalized loading of proteins.

the induction of the osteocalcin expression by FK506 is blocked by Smad6; the effect of FK506 on BMP signaling is additive rather than synergistic; FK506 rapidly induces the phosphorylation of the BMP-dependent Smads independently of the BMPs, and the induction is blocked by Smad6; and the activation of the Smads by FK506, but not that by BMP2, is attenuated by FKBP12, and the binding of FKBP12 to the BMP receptors is suppressed by FK506.

Although FK506 was reported to induce the ALP activity in some cultured cells and to enhance the osteocalcin mRNA expression induced by the BMPs [12], it was never demonstrated that FK506 alone was able to induce the osteocalcin expression. While the osteocalcin expression is highly specific to osteoblasts, the ALP activity is not. For example, the prehypertrophic and hypertrophic chondrocytes of the growth plate express a considerable amount of ALP [26], but not osteocalcin. Therefore, the effect of FK506 alone on the indisputable osteogenic differentiation remained unclarified. We demonstrated that FK506 alone at a higher concentration (1 μM) was able to induce the osteocalcin mRNA expression.

The high-turnover osteopenia was reported to be caused in mice, rats, and humans by the systemic administration of FK506 at approximately 0.01 μM and that of CsA at approximately 0.1 μM, which are clinical dosages used for the induction of immunosuppression [9,27,28]. At these concentrations, both FK506 and CsA inhibit calcineurin, similarly leading to a reduced function of the T cells [6]. Since FK506 inhibits nuclear factor of activated T cells (NFAT), an essential molecule for osteoclast differentiation, through inactivating calcineurin, FK506 is expected to decrease the number of osteoclasts. Both drugs, however, were reported to increase bone resorption by promoting the stromal cell RANKL expression and consequent osteoclast differentiation [29–31]. Further study is required to clarify this inconsistency. Our results showed that osteogenic differentiation as indicated by the osteocalcin mRNA expression was induced by FK506 at 1 μM, but not by CsA at the concentrations tested, strongly suggesting that this induction is independent of the inhibition of calcineurin and that FK506 at higher concentrations may have an additional downstream signaling pathway for osteogenic differentiation. We demonstrate that BMP signaling is such a pathway.

FK506 exerts its immunosuppressive effects via binding to FKBP12 [5]. We hypothesized that the osteogenic signal induced by FK506 might also involve FKBP12, which was reported to inhibit the ligand-independent signal from the BMPRIA. Our results show that BMPRIA and FKBP12 bound to each other, and that the overexpression of FKBP12 suppressed the activation of Smad signaling by FK506. These data suggest that FK506 may activate BMP signaling by competing for the binding site of FKBP12 with the BMP receptors. Alternatively, FK506 may be able to directly activate the BMP receptors, and FKBP12 may inhibit Smad signaling by sequestering FK506. Since FK506 dissociated FKBP12 from the BMPRIA, we find the first possibility more likely. This competitive interrelationship of FK506 and FKBP12 during osteogenic differentiation contrasts with the cooperative one during immunosuppression, in which FK506 and FKBP12 form a complex and exert the effect. As for the interaction between FK506 and BMP, the BMP2-induced phosphorylation of Smad1/5/8 was increased by addition of FK506. However, overexpression of FKBP12 did not affect the BMP2-induced phosphorylation of Smad1/5/8. We speculate that although FKBP12 blocks the ligand-independent activation of the BMPRI, it may not be able to bind and suppress the BMP-activated BMPRI (see Fig. 5).

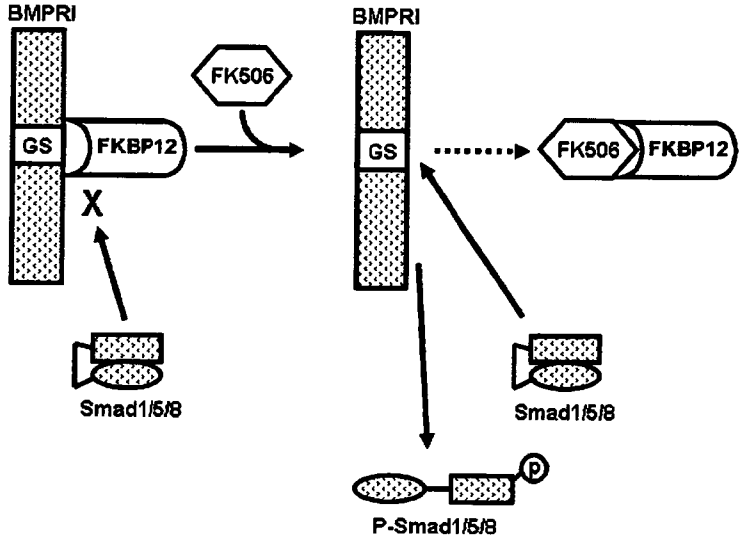

Fig. 5. Schematic representation of BMP signal activation by FK506. Based on the above-mentioned results, we propose the following model. FKBP12 binds to the BMPRI, stabilizes the inactive conformation, and blocks the ligand-independent activation of the receptors (left). FK506 competes for the GS region of the BMPRI with FKBP12 and allows the ligand-independent phosphorylation of the BMP-dependent Smads (right).

Recently, it has been reported that FK506 inhibits the osteoblast differentiation and function by suppressing expression of Runx2 and osterix mRNAs in ROS 17/2.8 cells [32] and by attenuating osterix function through NFAT signaling without changing expression of Runx2 mRNA [9]. These complex and confusing effects on the osteogenic differentiation by FK506 may be derived from the compound effects of FK506 on NFAT and BMP signalings. Although FK506 at the concentrations for immunosuppression mainly inhibits ostegenic differentiation by attenuating osterix function through regulating NFAT [9], FK506 at higher concentrations induces osteogenic differentiation by stimulating BMP/Smad signaling through regulating the interactions between BMPRI and FKBP12.

In conclusion, FK506 promotes osteogenic differentiation by activating the BMP receptors, probably through segregating them from FKBP12. In bone regenerative medicine, BMPs have been clinically used for treating intractable fractures and for spinal fusion [33–35]. The treatment, however, requires a large amount of expensive recombinant BMPs, thus hindering this method from becoming widely available. The osteogenic effect of FK506 at 1 μM roughly corresponds to that of BMP at 100 ng/ml. Provided that its systemic adverse effect can be avoided, the local use of FK506 as a surrogate for BMPs may help reduce the cost and may help broaden the application of bone regenerative medicine.

Acknowledgments

We thank Dr. K. Miyazono for the adenoviruses expressing LacZ and Smad6, the plasmids expressing HA-tagged BMPRIA and Flag-tagged FKBP12, and the 12xGCCG-luc reporter plasmid construct. This work was supported by a Grant-in-Aid for Scientific Research from the Japanese Ministry of Education, Culture, Sports, Science and Technology (#16659400).

References

[1] F. Vincenti, S.C. Jensik, R.S. Filo, J. Miller, J. Pirsch, A long-term comparison of tacrolimus (FK506) and cyclosporine in kidney transplantation: evidence for improved allograft survival at five years, Transplantation 73 (2002) 775–782.

[2] J.D. Pirsch, J. Miller, M.H. Deierhoi, F. Vincenti, R.S. Filo, A comparison of tacrolimus (FK506) and cyclosporine for immunosuppression after cadaveric renal transplantation. FK506 Kidney Transplant Study Group, Transplantation 63 (1997) 977–983.

[3] A.D. Mayer, J. Dmitrewski, J.P. Squifflet, T. Besse, B. Grabensee, B. Klein, F.W. Eigler, U. Heemann, R. Pichlmayr, M. Behrend, Y. Vanrenterghem, J. Donck, J. van Hooff, M. Christiaans, J.M. Morales, A. Andres, R.W. Johnson, C. Short, B. Buchholz, N. Rehmert, W. Land, S. Schleibner, J.L. Forsythe, D. Talbot, E. Pohanka, et al., Multicenter randomized trial comparing tacrolimus (FK506) and cyclosporine in the prevention of renal allograft rejection: a report of the European Tacrolimus Multicenter Renal Study Group, Transplantation 64 (1997) 436–443.

[4] J. Miller, Tacrolimus and mycophenolate mofetil in renal transplant recipients: one year results of a multicenter, randomized dose ranging trial. FK506/MMF Dose-Ranging Kidney Transplant Study Group, Transplant Proc. 31 (1999) 276–277.

[5] J. Liu, J.D. Farmer Jr., W.S. Lane, J. Friedman, I. Weissman, S.L. Schreiber, Calcineurin is a common target of cyclophilin-cyclosporin A and FKBP-FK506 complexes, Cell 66 (1991) 807–815.

[6] S.J. O'Keefe, J. Tamura, R.L. Kincaid, M.J. Tocci, E.A. O'Neill, FK-506- and CsA-sensitive activation of the interleukin-2 promoter by calcineurin, Nature 357 (1992) 692–694.

[7] K.M. Park, J.E. Hay, S.G. Lee, Y.J. Lee, R.H. Wiesner, M.K. Porayko, R.A. Krom, Bone loss after orthotopic liver transplantation: FK 506 versus cyclosporine, Transplant Proc. 28 (1996) 1738–1740.

[8] H.U. Stempfle, C. Werner, S. Echtler, T. Assum, B. Meiser, C.E. Angermann, K. Theisen, R. Gartner, Rapid trabecular bone loss after cardiac transplantation using FK506 (tacrolimus)-based immunosuppression, Transplant Proc. 30 (1998) 1132–1133.

[9] T. Koga, Y. Matsui, M. Asagiri, T. Kodama, B. de Crombrugghe, K. Nakashima, H. Takayanagi, NFAT and Osterix cooperatively regulate bone formation, Nat. Med. 11 (2005) 880–885.

[10] M. Cvetkovic, G.N. Mann, D.F. Romero, X.G. Liang, Y. Ma, W.S. Jee, S. Epstein, The deleterious effects of long-term cyclosporine A, cyclosporine G, and FK506 on bone mineral metabolism in vivo, Transplantation 57 (1994) 1231–1237.

[11] T. Inoue, I. Kawamura, M. Matsuo, M. Aketa, M. Mabuchi, J. Seki, T. Goto, Lesser reduction in bone mineral density by the immunosuppressant, FK506, compared with cyclosporine in rats, Transplantation 70 (2000) 774–779.

[12] L. Tang, S. Ebara, S. Kawasaki, S. Wakabayashi, T. Nikaido, K. Takaoka, FK506 enhanced osteoblastic differentiation in mesenchymal cells, Cell Biol. Int. 26 (2002) 75–84.

[13] S. Kaihara, K. Bessho, Y. Okubo, J. Sonobe, K. Kusumoto, Y. Ogawa, T. Iizuka, Effect of FK506 on osteoinduction by recombinant human bone morphogenetic protein-2, Life Sci. 72 (2002) 247–256.

[14] S. Kaihara, K. Bessho, Y. Okubo, J. Sonobe, M. Kawai, T. Iizuka, Simple and effective osteoinductive gene therapy by local injection of a bone morphogenetic protein-2-expressing recombinant adenoviral vector and FK506 mixture in rats, Gene Ther. 11 (2004) 439–447.

[15] M.R. Urist, Bone: formation by autoinduction, Science 150 (1965) 893–899.

[16] J.M. Wozney, V. Rosen, A.J. Celeste, L.M. Mitsock, M.J. Whitters, R.W. Kriz, R.M. Hewick, E.A. Wang, Novel regulators of bone formation: molecular clones and activities, Science 242 (1988) 1528–1534.

[17] M. Kawabata, K. Miyazono, Bone morphogenetic proteins, in: M.D. Ernesto Canalis (Ed.), Skeletal Growth Factors, Lippincott Williams & Wilkins, Philadelphia, 2000, pp. 269–290.

[18] J.L. Wrana, L. Attisano, MAD-related proteins in TGF-beta signalling, Trends Genet. 12 (1996) 493–496.

[19] C. Gruendler, Y. Lin, J. Farley, T. Wang, Proteasomal degradation of Smad1 induced by bone morphogenetic proteins, J. Biol. Chem. 276 (2001) 46533–46543.

[20] V. Rosen, J. Nove, J.J. Song, R.S. Thies, K. Cox, J.M. Wozney, Responsiveness of clonal limb bud cell lines to bone morphogenetic protein 2 reveals a sequential relationship between cartilage and bone cell phenotypes, J. Bone Miner. Res. 9 (1994) 1759–1768.

[21] T. Katagiri, A. Yamaguchi, M. Komaki, E. Abe, N. Takahashi, T. Ikeda, V. Rosen, J.M. Wozney, A. Fujisawa-Sehara, T. Suda, Bone morphogenetic protein-2 converts the differentiation pathway of C2C12 myoblasts into the osteoblast lineage, J. Cell Biol. 127 (1994) 1755–1766.

[22] K. Kusanagi, H. Inoue, Y. Ishidou, H.K. Mishima, M. Kawabata, K. Miyazono, Characterization of a bone morphogenetic protein-responsive Smad-binding element, Mol. Biol. Cell 11 (2000) 555–565.

[23] A. Hollnagel, V. Oehlmann, J. Heymer, U. Ruther, A. Nordheim, Id genes are direct targets of bone morphogenetic protein induction in embryonic stem cells, J. Biol. Chem. 274 (1999) 19838–19845.

[24] D.W. Jayme, K.E. Blackman, Culture media for propagation of mammalian cells, viruses, and other biologicals, Adv. Biotechnol. Processes 5 (1985) 1–30.
[25] M. Huse, Y.G. Chen, J. Massague, J. Kuriyan, Crystal structure of the cytoplasmic domain of the type I TGF beta receptor in complex with FKBP12, Cell 96 (1999) 425–436.
[26] H. Chikuda, F. Kugimiya, K. Hoshi, T. Ikeda, T. Ogasawara, T. Shimoaka, H. Kawano, S. Kamekura, A. Tsuchida, N. Yokoi, K. Nakamura, K. Komeda, U.I. Chung, H. Kawaguchi, Cyclic GMP-dependent protein kinase II is a molecular switch from proliferation to hypertrophic differentiation of chondrocytes, Genes Dev. 18 (2004) 2418–2429.
[27] R.P. Kershner, W.E. Fitzsimmons, Relationship of FK506 whole blood concentrations and efficacy and toxicity after liver and kidney transplantation, Transplantation 62 (1996) 920–926.
[28] J. Fryer, R.W. Yatscoff, E.A. Pascoe, J. Thliveris, The relationship of blood concentrations of rapamycin and cyclosporine to suppression of allograft rejection in a rabbit heterotopic heart transplant model, Transplantation 55 (1993) 340–345.
[29] C. Movsowitz, S. Epstein, F. Ismail, M. Fallon, S. Thomas, Cyclosporin A in the oophorectomized rat: unexpected severe bone resorption, J. Bone Miner. Res. 4 (1989) 393–398.
[30] L.C. Hofbauer, C. Shui, B.L. Riggs, C.R. Dunstan, T.C. Spelsberg, T. O'Brien, S. Khosla, Effects of immunosuppressants on receptor activator of NF-kappaB ligand and osteoprotegerin production by human osteoblastic and coronary artery smooth muscle cells, Biochem. Biophys. Res. Commun. 280 (2001) 334–339.
[31] J. Fukunaga, T. Yamaai, E. Yamachika, Y. Ishiwari, H. Tsujigiwa, K. Sawaki, Y.J. Lee, T. Ueno, S. Kirino, N. Mizukawa, S. Takagi, N. Nagai, T. Sugahara, Expression of osteoclast differentiation factor and osteoclastogenesis inhibitory factor in rat osteoporosis induced by immunosuppressant FK506, Bone 34 (2004) 425–431.
[32] S.S. Varanasi, H.K. Datta, Characterisation of cytosolic FK506 binding protein 12 and its role in modulating expression of Cbfa1 and osterix in ROS 17/2.8 cells, Bone 36 (2005) 243–253.
[33] S. Govender, C. Csimma, H.K. Genant, A. Valentin-Opran, Y. Amit, R. Arbel, H. Aro, D. Atar, M. Bishay, M.G. Borner, P. Chiron, P. Choong, J. Cinats, B. Courtenay, R. Feibel, B. Geulette, C. Gravel, N. Haas, M. Raschke, E. Hammacher, D. van der Velde, P. Hardy, M. Holt, C. Josten, R.L. Ketterl, B. Lindeque, G. Lob, H. Mathevon, G. McCoy, D. Marsh, R. Miller, E. Munting, S. Oevre, L. Nordsletten, A. Patel, A. Pohl, W. Rennie, P. Reynders, P.M. Rommens, J. Rondia, W.C. Rossouw, P.J. Daneel, S. Ruff, A. Ruter, S. Santavirta, T.A. Schildhauer, C. Gekle, R. Schnettler, D. Segal, H. Seiler, R.B. Snowdowne, J. Stapert, G. Taglang, R. Verdonk, L. Vogels, A. Weckbach, A. Wentzensen, T. Wisniewski, Recombinant human bone morphogenetic protein-2 for treatment of open tibial fractures: a prospective, controlled, randomized study of four hundred and fifty patients, J. Bone Joint Surg. Am. 84-A (2002) 2123–2134.
[34] S.D. Boden, J. Kang, H. Sandhu, J.G. Heller, Use of recombinant human bone morphogenetic protein-2 to achieve posterolateral lumbar spine fusion in humans: a prospective, randomized clinical pilot trial: 2002 Volvo Award in clinical studies, Spine 27 (2002) 2662–2673.
[35] J.K. Burkus, E.E. Transfeldt, S.H. Kitchel, R.G. Watkins, R.A. Balderston, Clinical and radiographic outcomes of anterior lumbar interbody fusion using recombinant human bone morphogenetic protein-2, Spine 27 (2002) 2396–2408.